

April 2010

---

**Thermometry**

**EUROMET Project No 426**

# **Final Report**

## **Intercomparison of heat flux sensors**

---

Prepared by:

***E. TURZÓ-ANDRÁS, T. MAGYARLAKI, S. NÉMETH, T. KOVÁCS***

***MKEH (Hungarian Trade Licensing Office)  
Thermometry Department***

***Emese Turzó-András***  
e-mail: [thurzo-a@mkeh.hu](mailto:thurzo-a@mkeh.hu)  
phone: +36 1 458 5963  
fax: +36 1 458 5927

## CONTENT

1.	INTRODUCTION.....	3
2.	SCHEDULE OF THE PROJECT .....	4
3.	PARTICIPATING LABORATORIES .....	5
4.	PROTOCOL AND ORGANISATION OF THE PROJECT .....	7
5.	MEASUREMENT RESULTS .....	9
6.	EVALUATION OF THE EURAMET REFERENCE VALUE: ERV .....	23
7.	CONCLUSION .....	25
8.	REFERENCES .....	26
9.	APPENDIX A: DESCRIPTION OF THE MEASUREMENT SET-UP .....	27
10.	APPENDIX B: UNCERTAINTY EVALUATIONS .....	33

# 1. Introduction

The first intercomparison on density of heat flow rate measurements has been organized by MKEH (Hungarian Trade Licensing Office, Metrology Department).

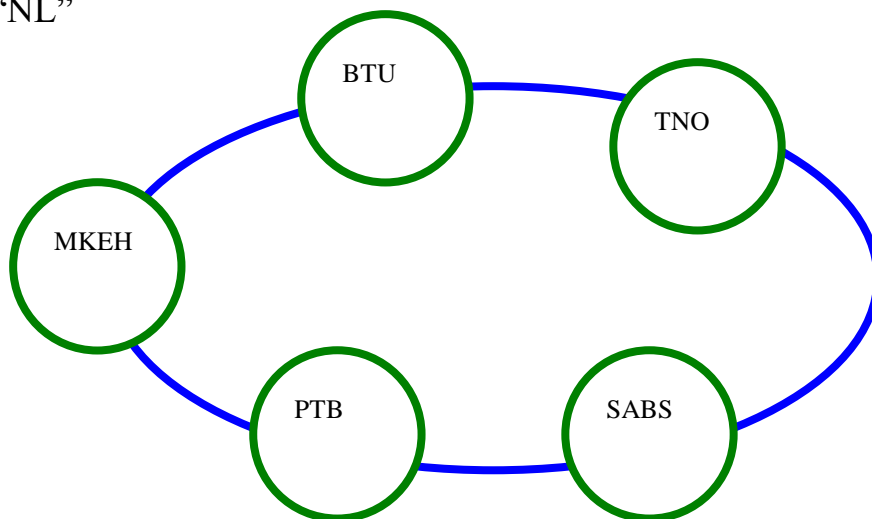
The objective of this round robin test was to improve the accuracy in the realisation of a density of heat flow rate scale up to  $100 \text{ W}\cdot\text{m}^{-2}$ .

Two types of heat flux plate sensors differing in their size and here denoted as “NL” and “HU” were circulated among five (NL) and two (HU) partner laboratories, respectively. Each one of the six partners calibrated the sensors using its individual heat source, a guarded hot plate or a heat flow meter apparatus. Measurements were performed at nominal temperatures of  $20 \text{ }^\circ\text{C}$  and  $30 \text{ }^\circ\text{C}$ .

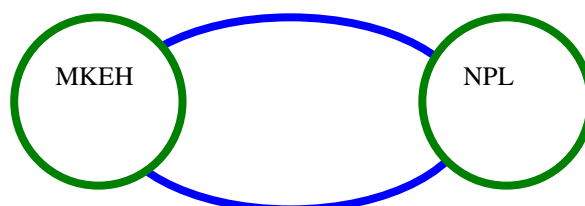
The report compares all the results of the round robin test and gives the mutual differences among the partners. Individual uncertainty estimations are presented in detail.

## Organisation of the comparison

Sensor “NL”



Sensor “HU”



## 2. Schedule of the project

For a given laboratory, the time allowed for the measurements was at least 8 month, including the travelling time between the laboratories. The circulation of the heat flux sensors was restarted three times. Due to delays caused by several reasons (for example retiring of the previous coordinator) the provisional schedule had to be changed several times.

Laboratory	Country code	Person responsible	Year of measurement
MKEH1	HU	T. Magyarlaki	2000
BTU	DE	S. Rudtsch	2000
TNO	NL	H. Blokland	2001
SABS	SA	C. Krös	2002
PTB	DE	U. Hammerschmidt	2004
MKEH2	HU	E. Turzo-Andras	2006

Table 1: *Schedule of the project in case of heat flux sensor “NL”*

Laboratory	Country code	Person responsible	Date of measurement
MKEH1	HU	T. Magyarlaki	2000
NPL	UK	D. Salmon	2001
MKEH2	HU	E. Turzo-Andras	2006

Table 2: *Schedule of the project in case of heat flux sensor “HU”*

### **3. Participating laboratories**

In alphabetic order the following NMIs participated in the project:  
BTU (DE), MKEH (HU), NPL (UK), PTB (DE), SABS (SA), TNO (NL)

Details for the laboratories are as follows:

#### **GERMANY (BTU)**

Steffen Rudtsch  
Brandenburg University of Technology Cottbus  
Applied Physics I / Thermophysics  
Konrad-Zuse-Str. 1  
03013 Cottbus  
Phone : + 49 30 3481 7650  
Fax : + 49 30 3481 7504  
Email : steffen.rudtsch@ptb.de

#### **GERMANY (PTB)**

Ulf Hammerschmidt  
Physikalisch-Technische-Bundesanstalt  
Bundesallee 100  
38116 Braunschweig  
Phone : + 49 531 592 3211  
Fax : + 49 531 592 3209  
Email : ulf.hammerschmidt@ptb.de

#### **HUNGARY (MKEH)**

Emese Turzo-Andras  
Hungarian Trade Licensing Office (MKEH)  
Metrology Department  
Németvölgyi út 37-39  
1124 Budapest  
Phone + 36 1 458 5963  
Fax: + 36 1 458 5983  
email: thurzo-a@mkeh.hu

**The NETHERLANDS (TNO)**

Huib Blokland  
TNO Science & Industry  
P. O. Box 155  
2600 AD Delft  
Phone: + 31 15 269 2108  
Fax : + 31 15 269 2111  
Email : huib.blokland@tno.nl

**SOUTH AFRICA (SABS)**

Charles Krös  
South African Bureau of Standards  
1 Dr Lategan Road  
Groenkloof  
Pretoria  
Phone : + 27 12 428 6690  
Fax : + 27 12 428 6214  
email : hendrih@sabs.co.za

**UNITED KINGDOM (NPL)**

Clark Stacey  
National Physical Laboratory  
Queens road  
Teddington  
Middlesex  
TW11 OLW  
United Kingdom  
Phone : + 44 20 8943 6578  
email : Clark.Stacey@npl.co.uk

## 4. Protocol and organisation of the project

### Transfer heat flux transducers

Two types of heat flux plate sensors having different dimensions, electrical resistance, sensitivity and thermal conductivity were circulated. They are illustrated in Fig. 1 and Fig. 2. The characteristics of the heat flux sensors are given in Table 2.

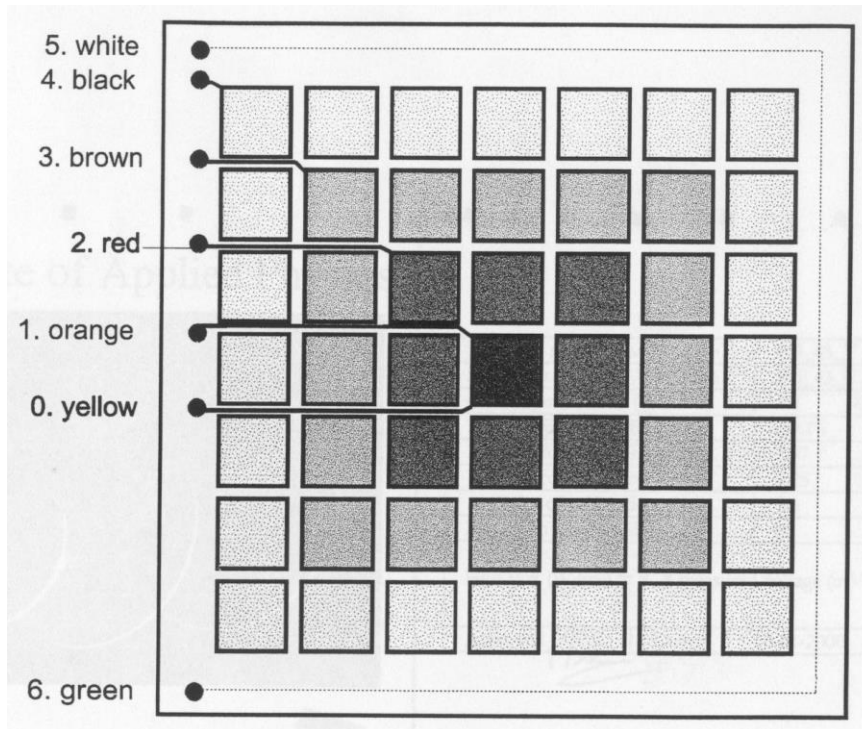
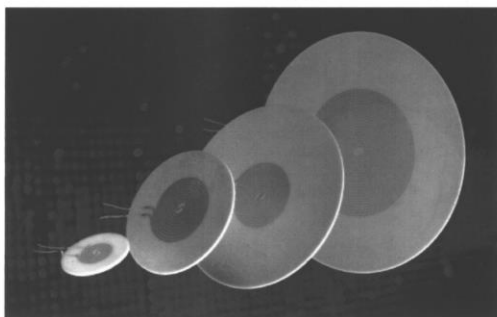


Fig. 1. Heat flux sensor “HU” (reference area: 100×100 mm, voltage output between red and yellow)

TNO Institute of Applied Physics



Heat Flux Sensor



Heat flux sensor type	PU_43_T	
Serial number	PU_43_T.0087	
Calibration value C (at 20 °C)	5.8	W/m <sup>2</sup> .mV
Temperature correction	+0.1	%/K
Internal electrical resistance	7.97	kOhm
Thermal conductivity	0.25	W/m.K
Accuracy of calibration value	5.0	%
Maximum temperature	60	°C
Heat flux (W/m <sup>2</sup> ) = C * measured voltage (mV)		
Approved		Date: 10-01-2000

Fig. 2. Heat flux sensor “NL” (reference area:  $\phi$  55 mm)

Table 3: *Particulars of the heat flux sensors*

<b>Sensor</b>	<b>No 1 “NL”</b>	<b>No 2 “HU”</b>
<b>Model</b>	PU 43 T	OMH 1
<b>Dimensions</b>	$\phi$ 100×1 mm	300×300×3.5 mm
<b>Sensitive area</b>	$\phi$ 55 mm	100×100 mm
<b>Sensitivity</b>	0.17 mV·m <sup>2</sup> /W	5...9 $\mu$ V·m <sup>2</sup> /W
<b>Electrical resistance</b>	7000 $\Omega$	6...24 $\Omega$
<b>Max. temperature</b>	60 °C	100 °C
<b>Thermal conductivity</b>	0.2 ÷ 0.3 W/m·K	0.3 ÷ 0.4 W/m·K
<b>Cable length</b>	2 m	2 m

## Measurement instruction and reporting

The objective of this round robin test was to improve the accuracy in the realisation of a density of heat flow rate scale up to 100 W·m<sup>-2</sup>.

Two types of heat flux plate sensors differing in their size and here denoted as “NL” and “HU” were circulated among five (NL) and two (HU) partner laboratories, respectively. Each one of the six partners calibrated one or both of the sensors, depending on the dimensions of their measurement apparatus, at nominal densities of heat flow rates of 10 W·m<sup>-2</sup>, 50 W·m<sup>-2</sup> and 100 W·m<sup>-2</sup>, using its individual heat source, a guarded hot plate or a heat flow meter apparatus. Measurements were performed at nominal temperatures of 20 °C and 30 °C. The first and last measurements were effectuated by the pilot laboratory MKEH.

Adjustment of the desired heat flow rate was achieved by modifying the temperature difference the upper and lower part of the sensor, for a given nominal temperature.

The calibration of the heat flux sensors was done using the following recommendations: ISO 9869:1994(E), ISO 8302:1991, ISO 8301:1991, ISO 7345:1987.



## 5. Measurement results

Measurements were performed with two types of heat flux plate sensors differing in their size, at nominal temperatures of 20 °C and 30 °C and at nominal densities of heat flow rates of 10 W·m<sup>-2</sup>, 50 W·m<sup>-2</sup> and 100 W·m<sup>-2</sup>.

The calibration procedure used involved determination of the realised densities of heat flow rates, measurement of the voltage outputs, evaluation of the sensitivities and their associated uncertainties.

The measurement results are grouped considering the two types of heat flux sensors and the two different nominal temperatures. The sensor “NL” was circulated among five partner laboratories. The sensor “HU” was circulated among two partner laboratories.

Table 4 and 5 summarises the reported results and the combined standard uncertainties given by the partner laboratories. The results are composed from the realised density of heat flow rate values, from reading values of the sensor output and from the calculated sensitivity values which are specific for one type of sensor.

Fig. 3, Fig. 5, Fig. 9 and Fig. 11 show the deviation curves in case of different sensors and temperatures.

The measurement results are compared in Fig. 4, Fig. 6, Fig. 10, Fig. 12.

Fig. 7, Fig. 8, Fig. 13 and Fig. 14 show the sensitivity values reported by the partner laboratories and the uncertainty bars (k=2) for the two different sensors, two different temperatures and three different densities of heat flow rate, respectively. The values of the median (—) and its uncertainty band (-----) are plotted on each graph.

The sensitivity was obtained by:

$$S_{lab} = \frac{U_{lab}}{q_{lab}} \quad [\mu V \cdot W^{-1} \cdot m^2] \quad (1)$$

where  $U_{lab}$  is the voltage of the heat flux sensor output measured by each partner

$q_{lab}$  is the density of heat flow rate given by the participants

Table 4. Reported results for the heat flux sensor “NL”

Table 4.1. Density of heat flow rate values for different laboratories

Sensor NL							
heat flux nominal [W/m <sup>2</sup> ]	sensor temperature (nominal) [°C]	realised heat flux [W/m <sup>2</sup> ] MKEH1	realised heat flux [W/m <sup>2</sup> ] PTB	realised heat flux [W/m <sup>2</sup> ] BTU	realised heat flux [W/m <sup>2</sup> ] TNO	realised heat flux [W/m <sup>2</sup> ] SABS	realised heat flux [W/m <sup>2</sup> ] MKEH2
10	20	9.81	9.49	10.52	6.69	10.59	9.81
10	30	11.49	9.33	9.74	7.06	11.02	10.13
50	20	53.25	47.24	51.02	30.95		53.96
50	30	51.06	48.66	50.13	26.52	27.94	49.22
100	20	99.28	96.21	102.94			103.52
100	30	100.29	97.35	101.02			100.66

Table 4.2. Heat flux transducer output for different laboratories

Sensor NL							
heat flux nominal [W/m <sup>2</sup> ]	sensor temperature (nominal) [°C]	reading [μV] MKEH1	reading [μV] PTB	reading [μV] BTU	reading [μV] TNO	reading [μV] SABS	reading [μV] MKEH2
10	20	1679.31	1622	1851.05	1132.2	1462.7	1679.20
10	30	1980.44	1632	1669.7	1206.6	1373.5	1758.54
50	20	9214.02	8143	8995.89	5276.3		9357.26
50	30	8778.45	8221	8788.48	4678.8	4397	8426.26
100	20	17149.48	16373	18148.68			17887.23
100	30	17254.01	16479	17747.98			17270.53

Table 4.3. Sensitivity values for different laboratories

Sensor NL							
heat flux nominal [W/ m <sup>2</sup> ]	sensor temperature (nominal) [°C]	sensitivity MKEH1 [μV/W/m <sup>2</sup> ]	sensitivity PTB [μV/W/m <sup>2</sup> ]	sensitivity BTU [μV/W/m <sup>2</sup> ]	sensitivity TNO [μV/W/m <sup>2</sup> ]	sensitivity SABS [μV/W/m <sup>2</sup> ]	sensitivity MKEH2 [μV/W/m <sup>2</sup> ]
10	20	171.27	170.917	175.96	169.3	138.1	171.26
10	30	172.39	174.920	171.43	171	124.6	173.53
50	20	173.05	172.375	176.32	170.5		173.41
50	30	171.91	168.948	175.31	176.4	157.4	171.19
100	20	172.74	170.180	176.30			172.79
100	30	172.04	169.276	175.69			171.57

Table 4.4. Uncertainty values for different laboratories

Sensor NL	heat flux nominal [W/m <sup>2</sup> ]	sensor temperature nominal [°C]	uncertainty MKEH1 [%]	uncertainty PTB [%]	uncertainty BTU [%]	uncertainty TNO [%]	uncertainty SABS [%]	uncertainty MKEH2 [%]
10	10	20	2.1	2.3	4.9	2.5	10.3	2.1
10	10	30	2.1	2.3	4.9	2.5	10.3	2.1
50	50	20	2.0	2.3	4.9	2.5		2.0
50	50	30	2.0	2.3	4.9	2.5	10.3	2.0
100	100	20	2.0	2.3	4.9			2.0
100	100	30	2.0	2.3	4.9			2.0

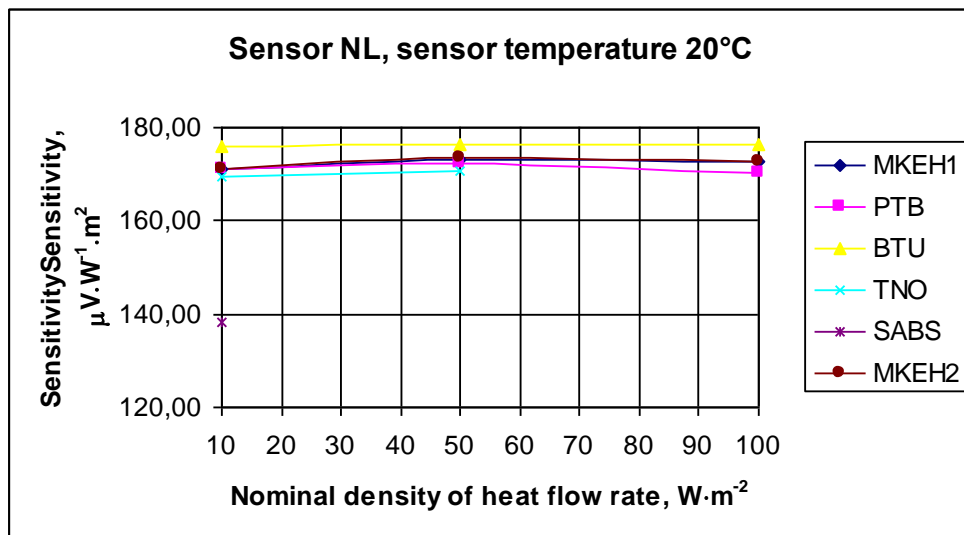


Fig. 3. Deviation curves for sensor “NL”, temperature 20°C

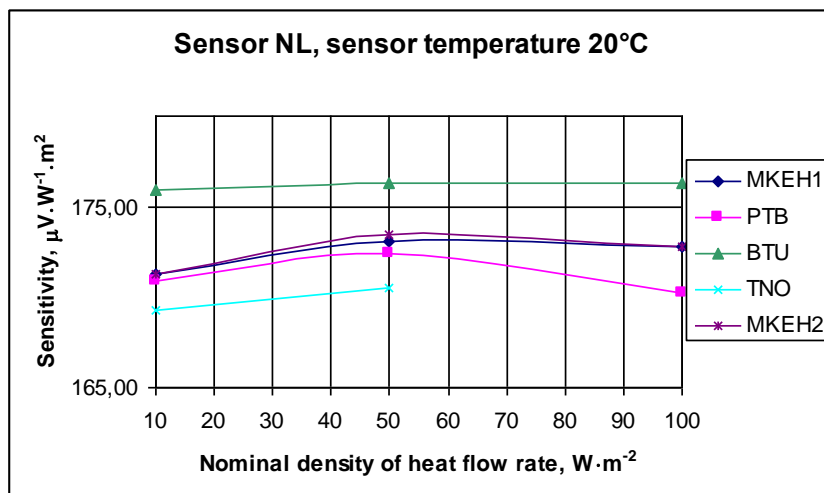


Fig. 3.1. Deviation curves for sensor “NL”, temperature 20°C, without the results of SABS

Fig. 4. Results for the sensor “NL”, sensor temperature 20°C

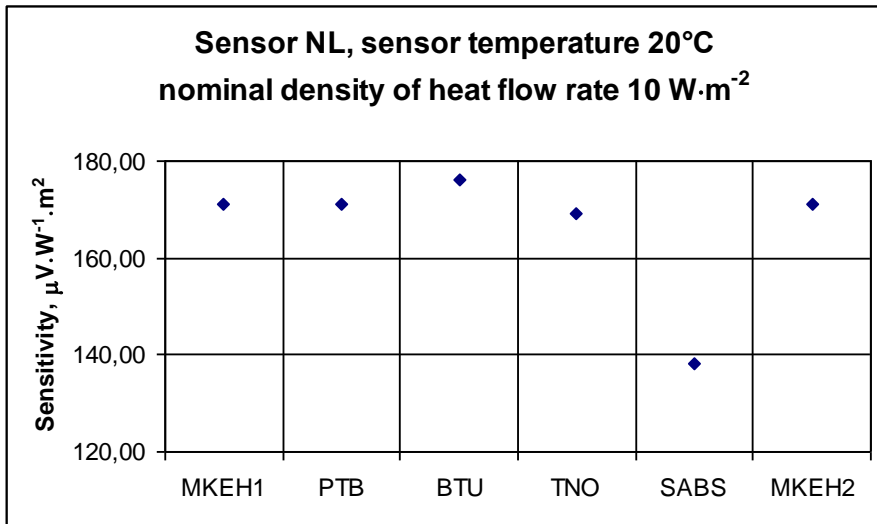


Fig. 4.1.

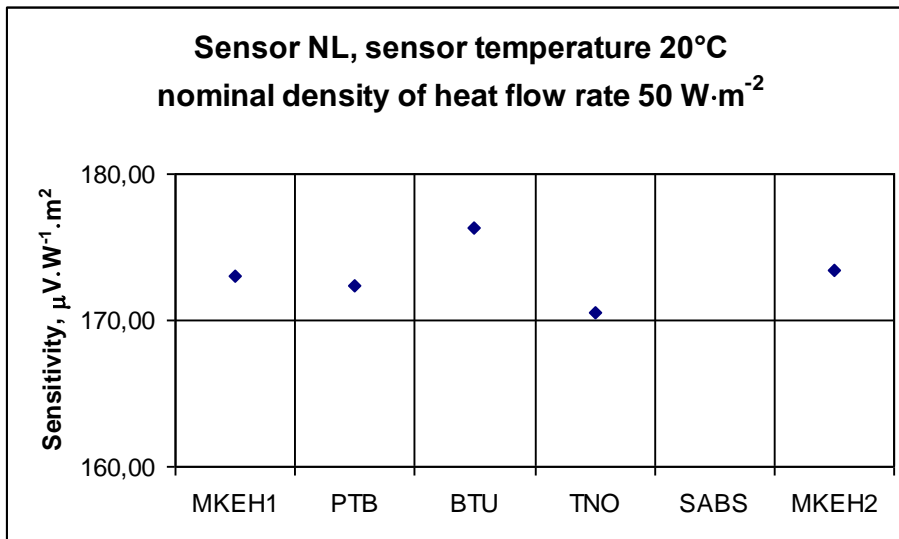


Fig. 4.2.

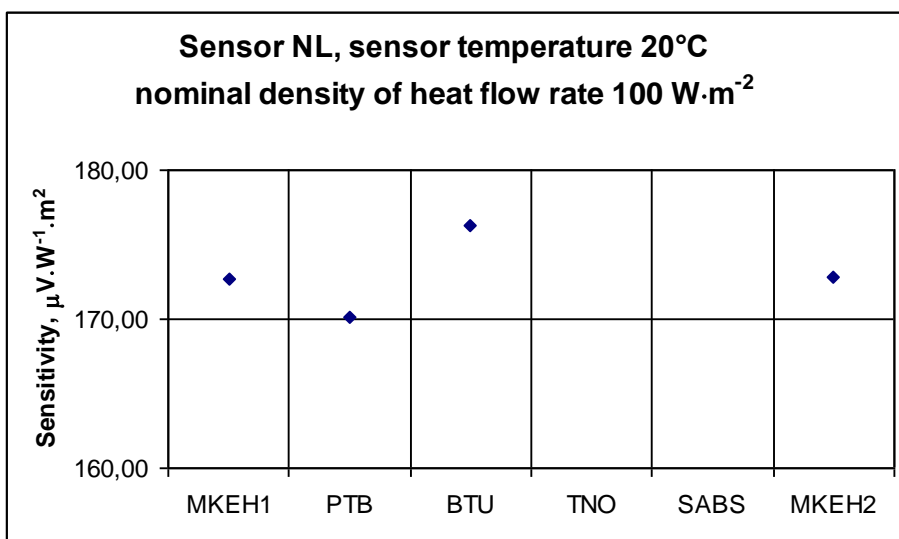


Fig. 4.3.

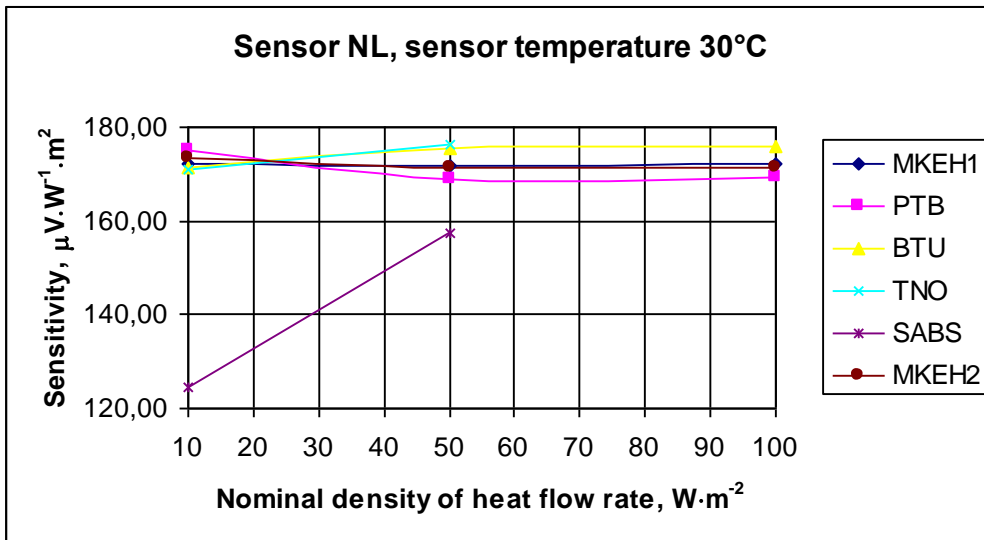


Fig. 5. Deviation curves for sensor "NL", temperature 30°C

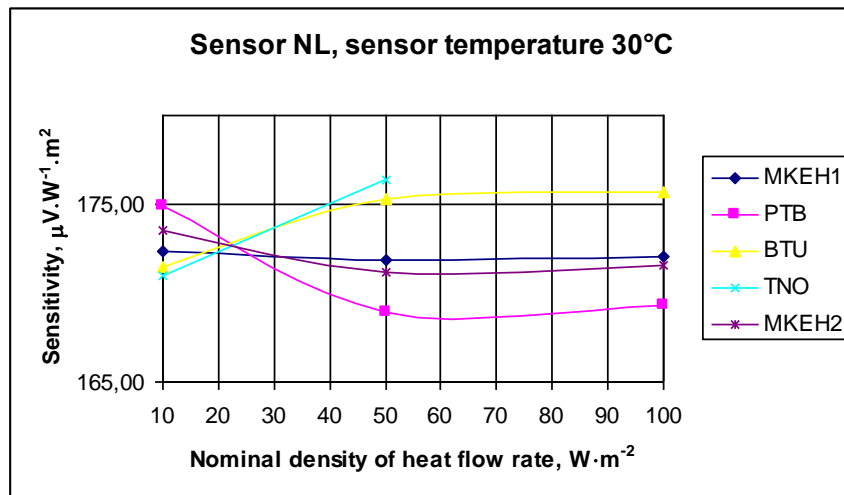


Fig. 5.1. Deviation curves for sensor "NL", temperature 30°C, without the results of SABS

Fig. 6. Results for the sensor "NL", sensor temperature 30°C

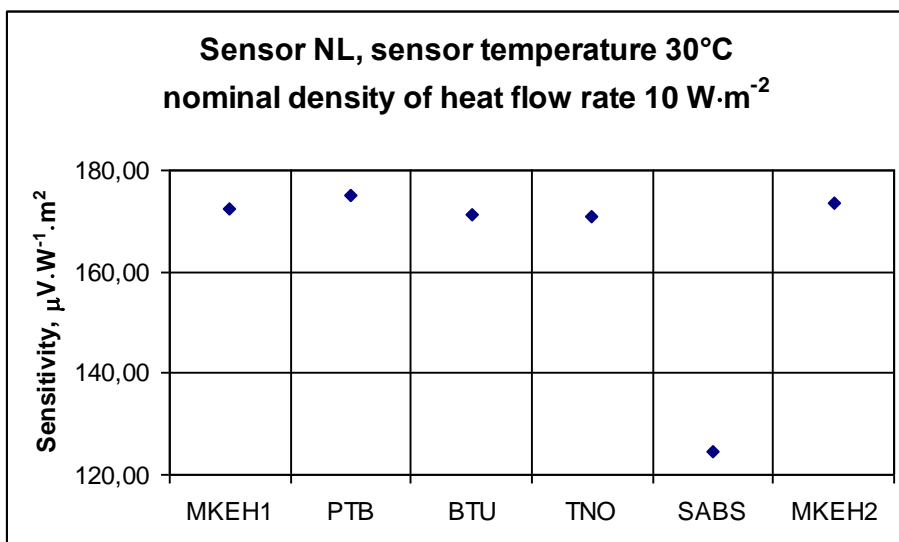


Fig. 6.1.

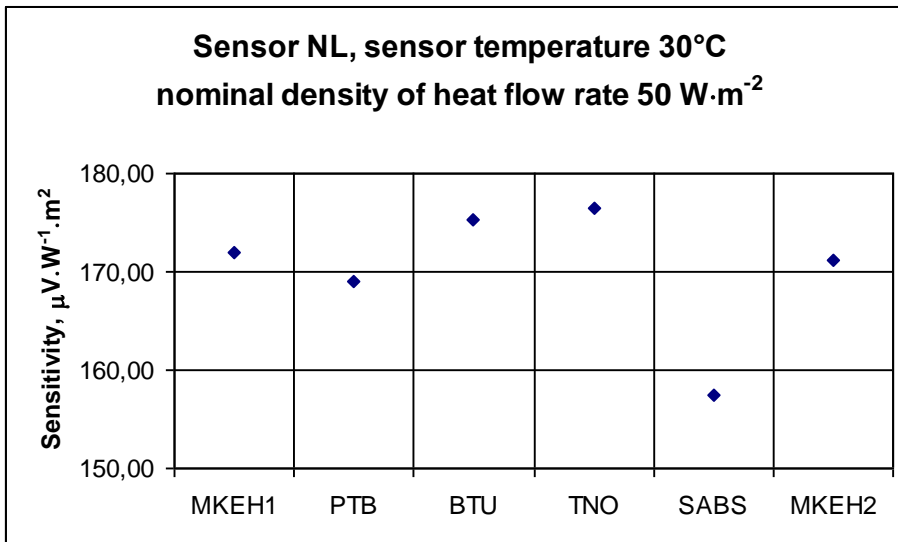


Fig. 6.2.

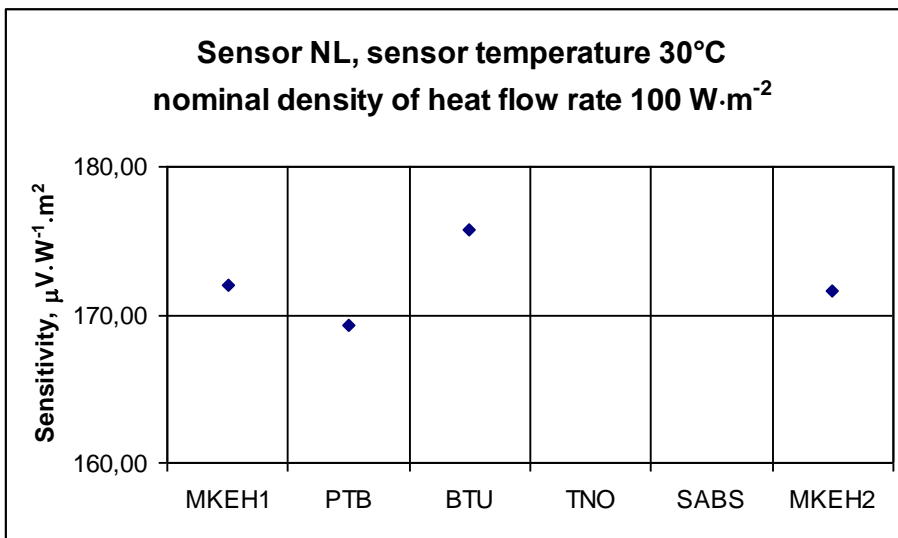


Fig. 6.3.

Fig. 7. Measurement results and uncertainties for the sensor “NL”, sensor temperature 20°C, reference value: median

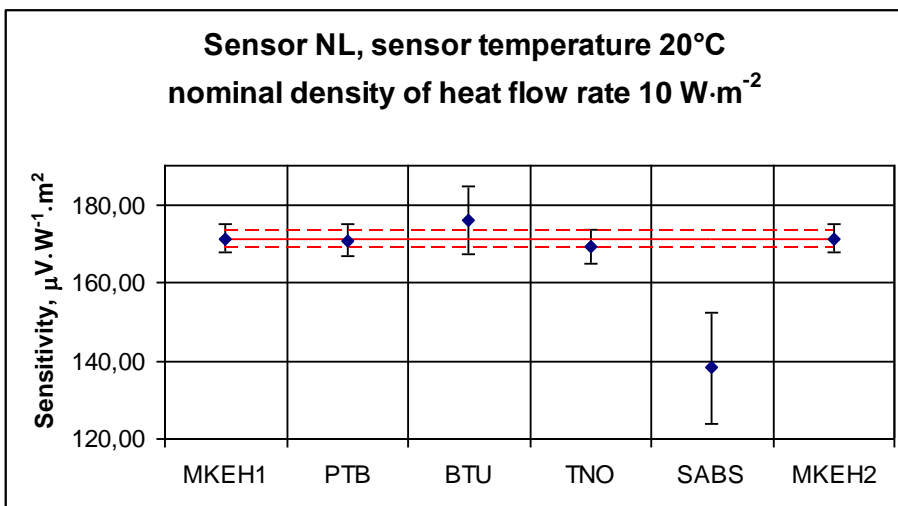


Fig. 7.1.

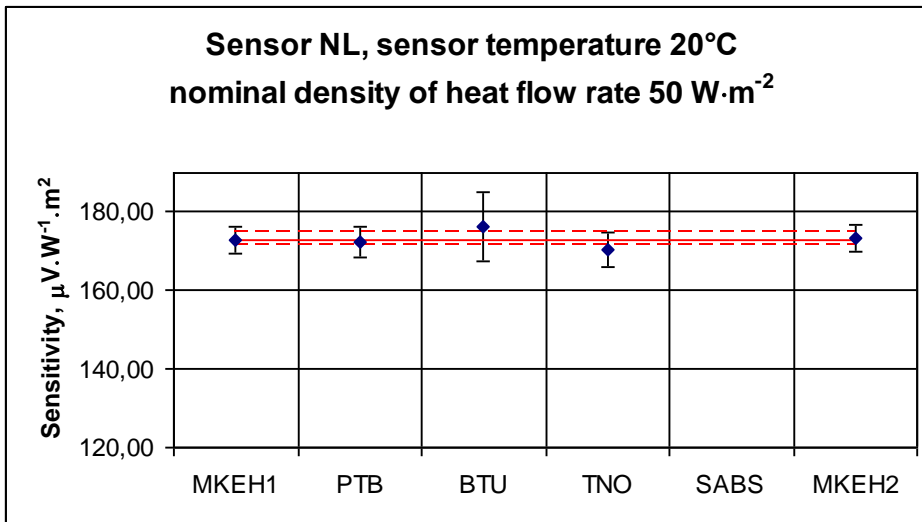


Fig. 7.2.

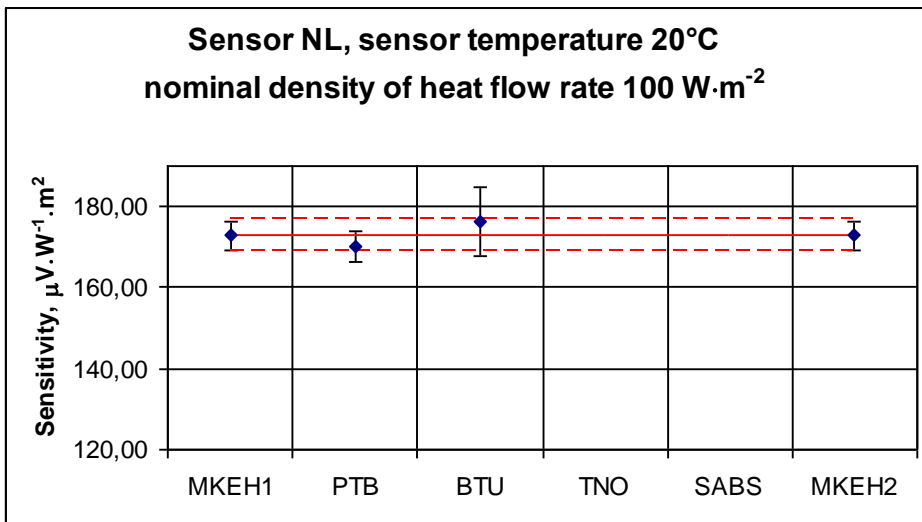


Fig. 7.3.

Fig. 8. Measurement results and uncertainties for the sensor “NL”, sensor temperature 30°C, reference value: median

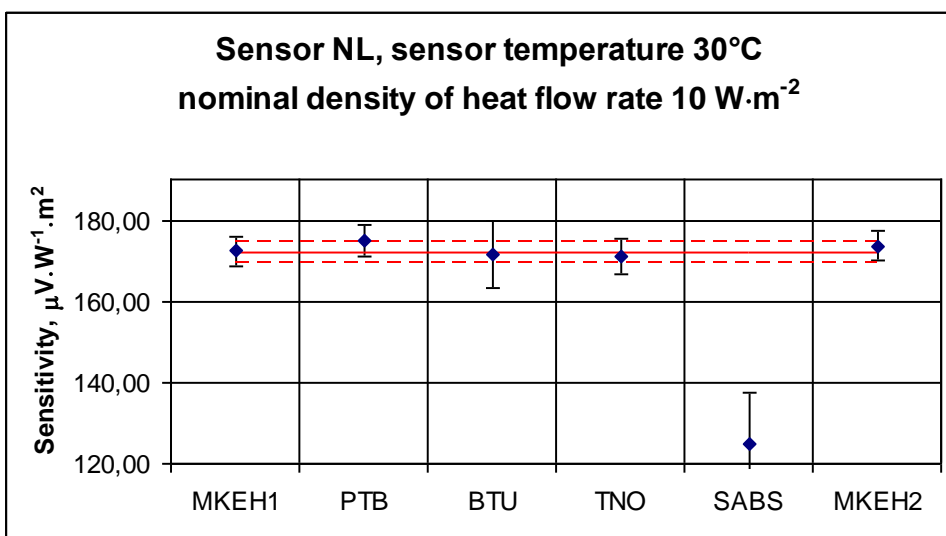


Fig. 8.1.

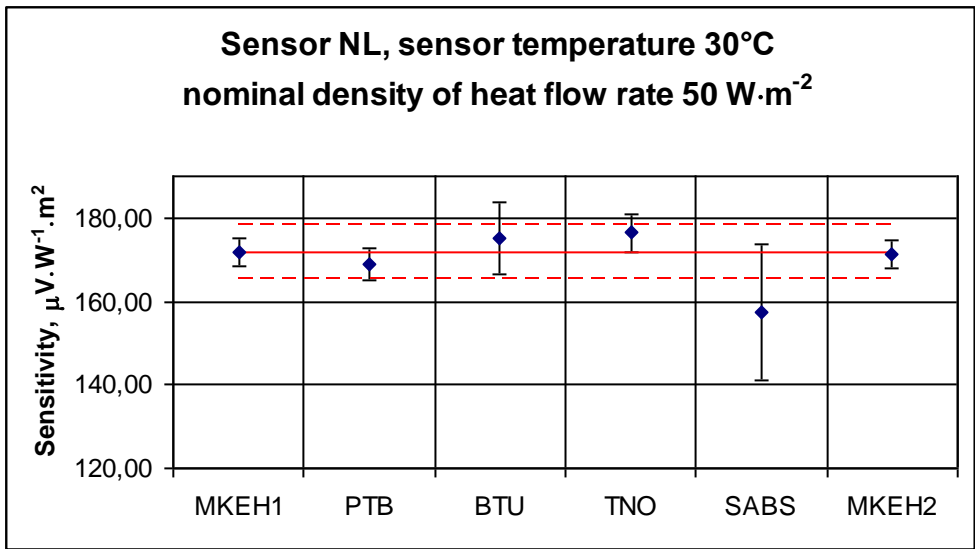


Fig. 8.2.

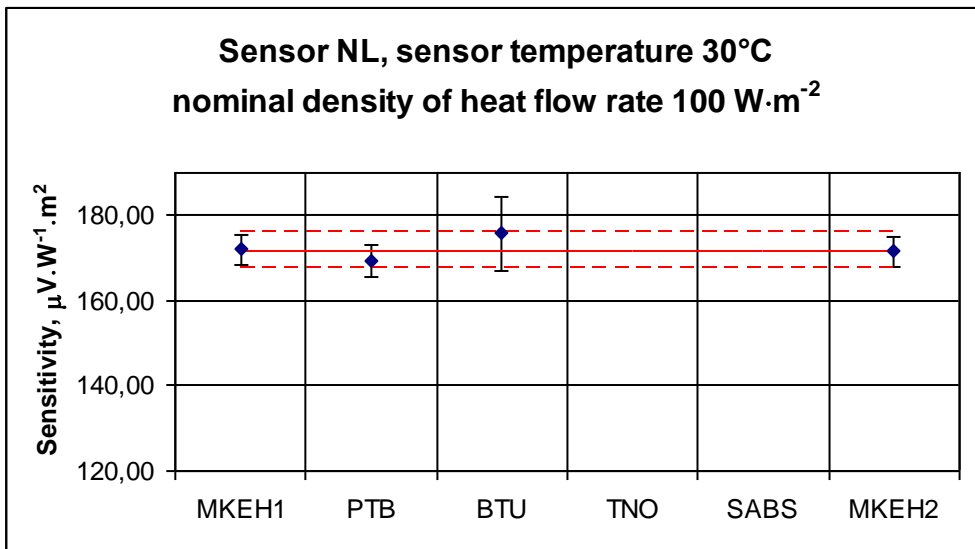


Fig. 8.3.

Table 5. Reported results for the heat flux sensor “HU”

Table 5.1. Density of heat flow rate values for different laboratories

Sensor HU				
heat flux nominal [W/m²]	sensor temp [°C]	realised heat flux [W/m²] MKEH1	realised heat flux [W/m²] NPL	realised heat flux [W/m²] MKEH2
10	20	11.01	10.08	10.80
10	30	9.25	9.90	13.16
50	20	52.46	50.34	50.65
50	30	52.72	49.49	51.91
100	20	100.05	100.02	100.42
100	30	102.98	98.37	100.09



Table 5.2. Heat flux transducer output for different laboratories

Sensor HU				
heat flux nominal [W/m <sup>2</sup> ]	sensor temp [°C]	reading [μV] MKEH1	reading [μV] NPL	reading [μV] MKEH2
10	20	65.50	62.4	66.66
10	30	56.30	59.6	78.41
50	20	316.45	300.0	302.13
50	30	321.05	299.1	317.23
100	20	600.77	590.3	604.34
100	30	627.15	591.2	600.77

Table 5.3. Sensitivity values for different laboratories

Sensor HU				
heat flux nominal [W/m <sup>2</sup> ]	sensor temp [°C]	sensitivity [μV/W/m <sup>2</sup> ] MKEH1	sensitivity [μV/W/m <sup>2</sup> ] NPL	sensitivity [μV/W/m <sup>2</sup> ] MKEH2
10	20	5.95	6.19	6.17
10	30	6.09	6.02	5.96
50	20	6.03	5.96	5.97
50	30	6.09	6.04	6.11
100	20	6.00	5.90	6.02
100	30	6.09	6.01	6.00

Table 5.4. Uncertainty values for different laboratories

Sensor HU				
heat flux nominal [W/m <sup>2</sup> ]	sensor temp [°C]	uncertainty [%] MKEH1	uncertainty [%] NPL	uncertainty [%] MKEH2
10	20	3.8	6.5	3.8
10	30	3.4	2.2	3.4
50	20	2.1	1.5	2.1
50	30	2.1	0.9	2.1
100	20	2.0	1.1	2.0
100	30	2.0	0.8	2.0

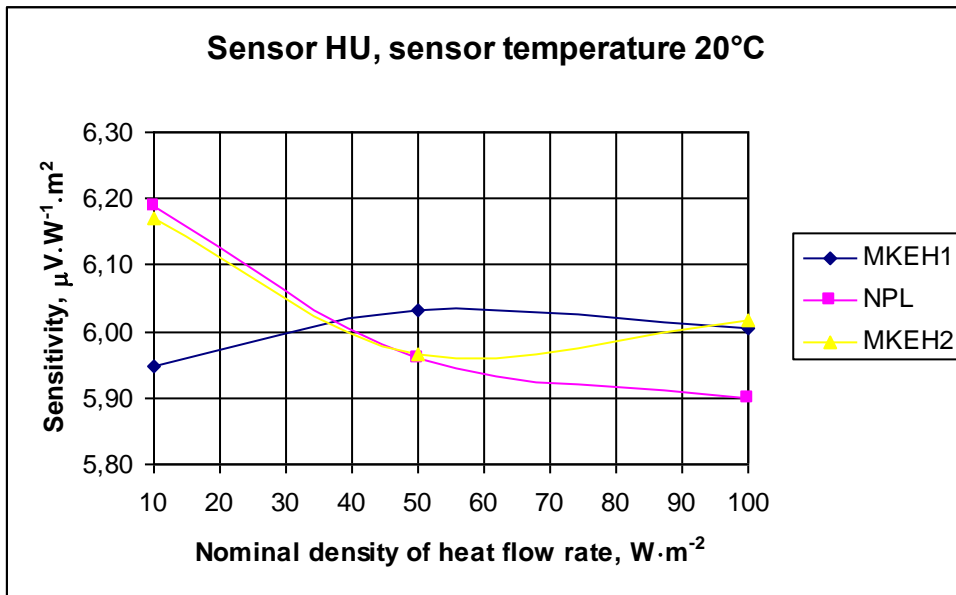


Fig. 9. Deviation curves for sensor “HU”, temperature 20°C

Fig. 10. Results for the sensor “HU”, sensor temperature 20°C

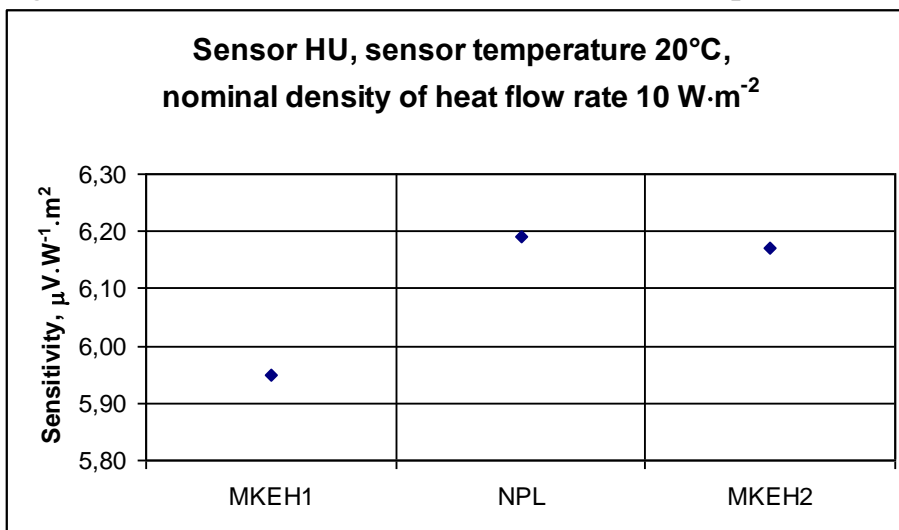


Fig. 10.1.

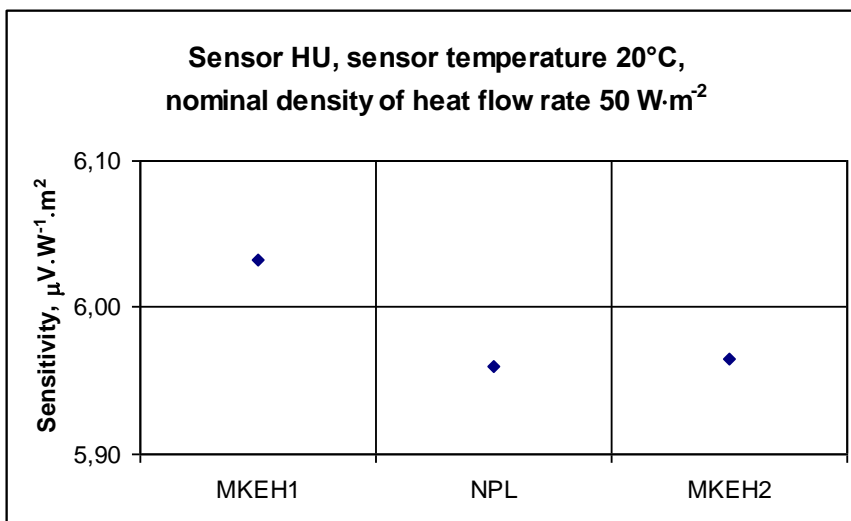


Fig. 10.2.

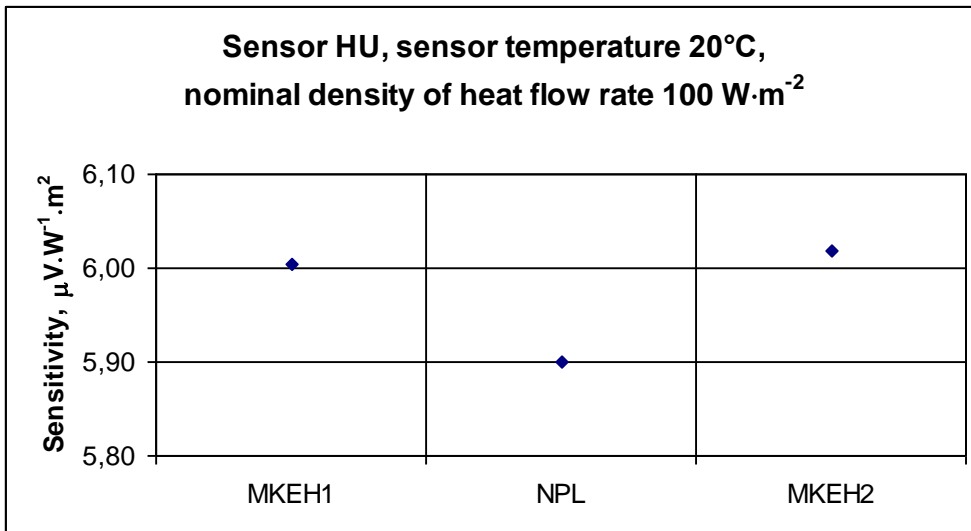


Fig. 10.3.

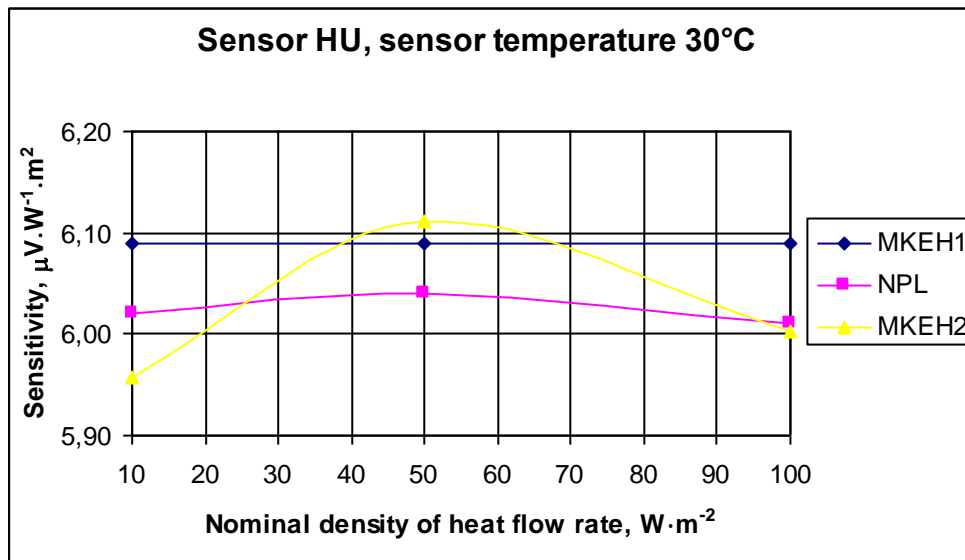


Fig. 11. Deviation curves for sensor “HU”, temperature 30°C

Fig. 12. Results for the sensor “HU”, sensor temperature 30°C

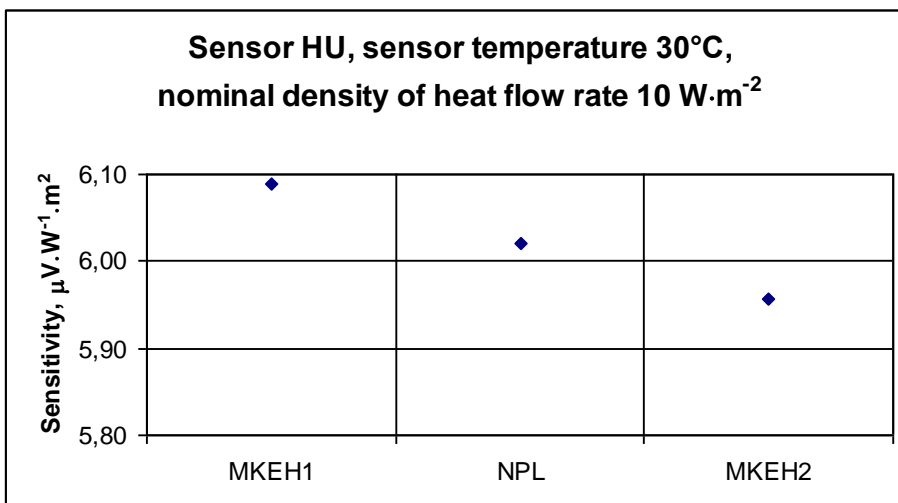


Fig. 12.1.

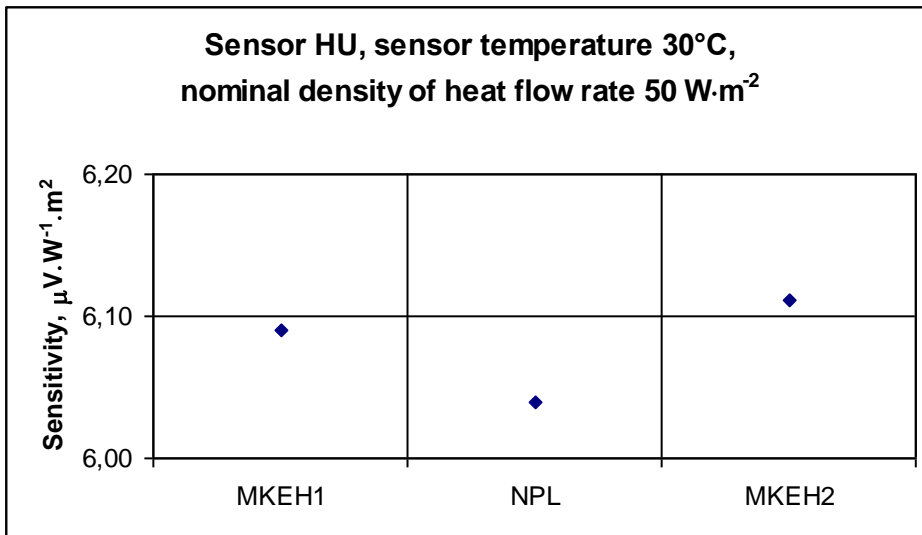


Fig. 12.2.

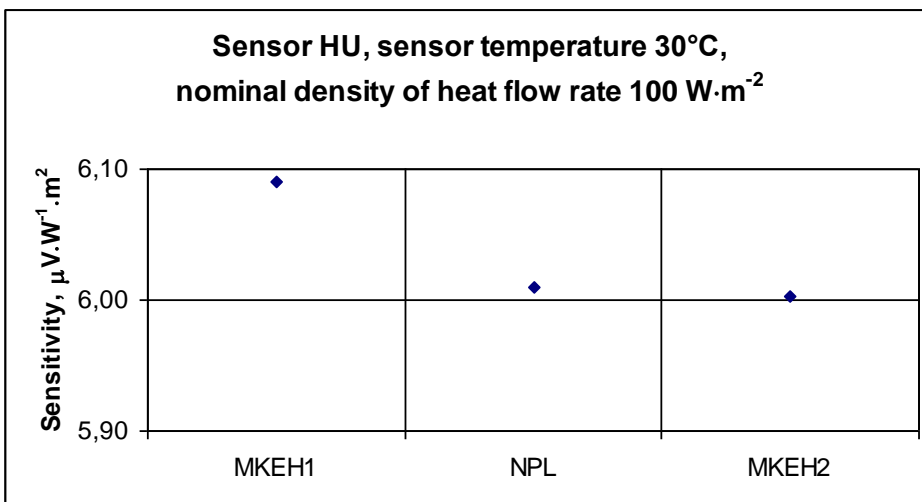


Fig. 12.3.

Fig. 13. Measurement results and uncertainties for the sensor “HU”, sensor temperature 20°C, reference value: median

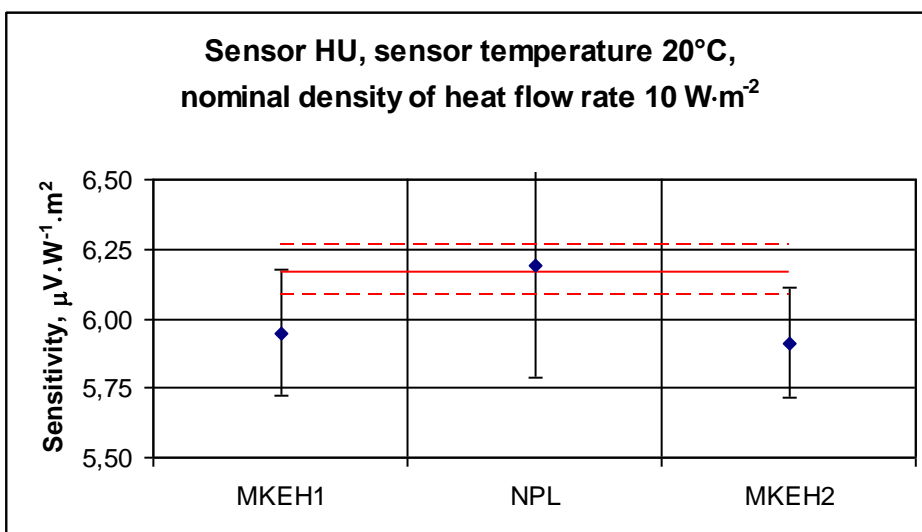


Fig. 13.1.

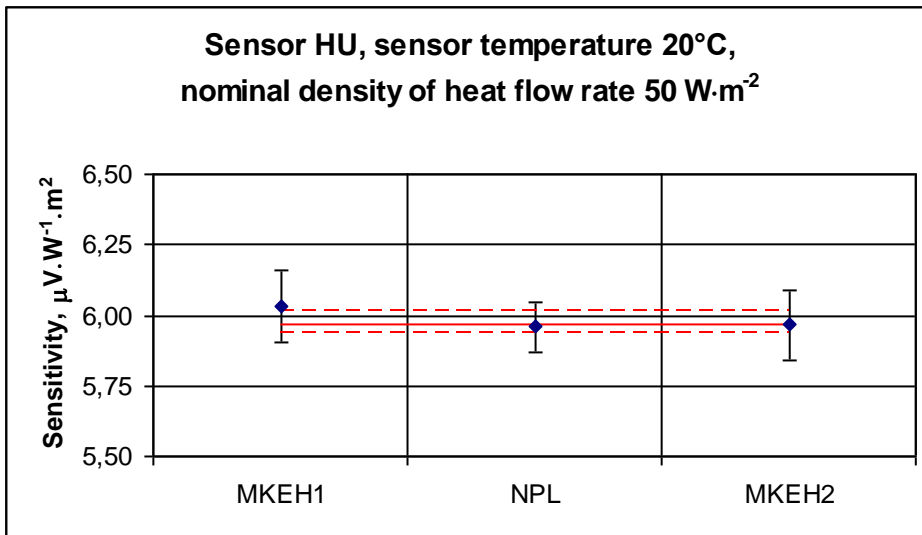


Fig. 13.2.

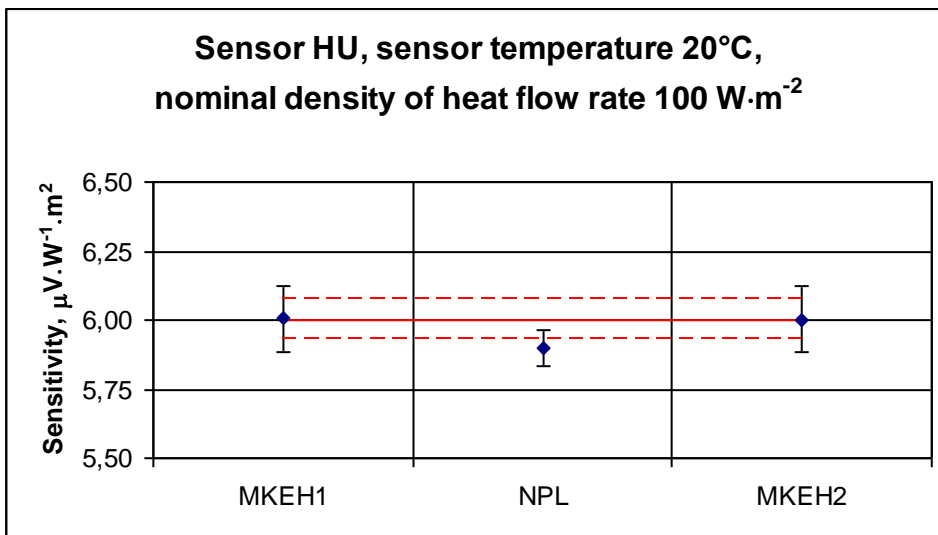


Fig. 13.3.

Fig. 14. Measurement results and uncertainties for the sensor “HU”, sensor temperature 30°C, reference value: median

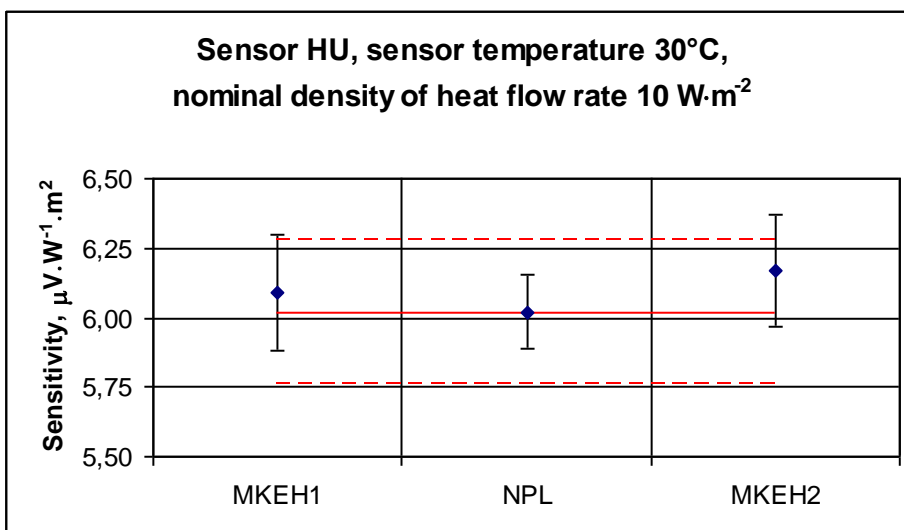


Fig. 14.1.

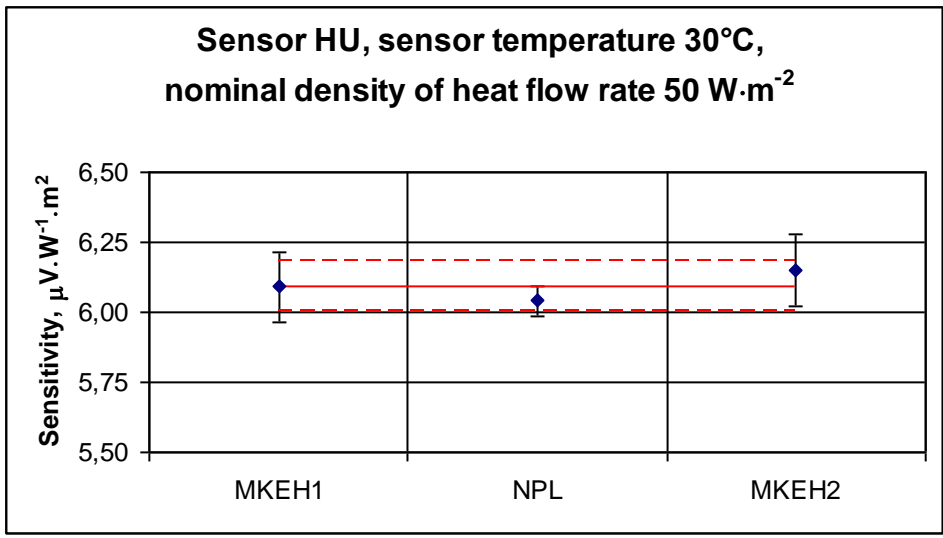


Fig. 14.2.

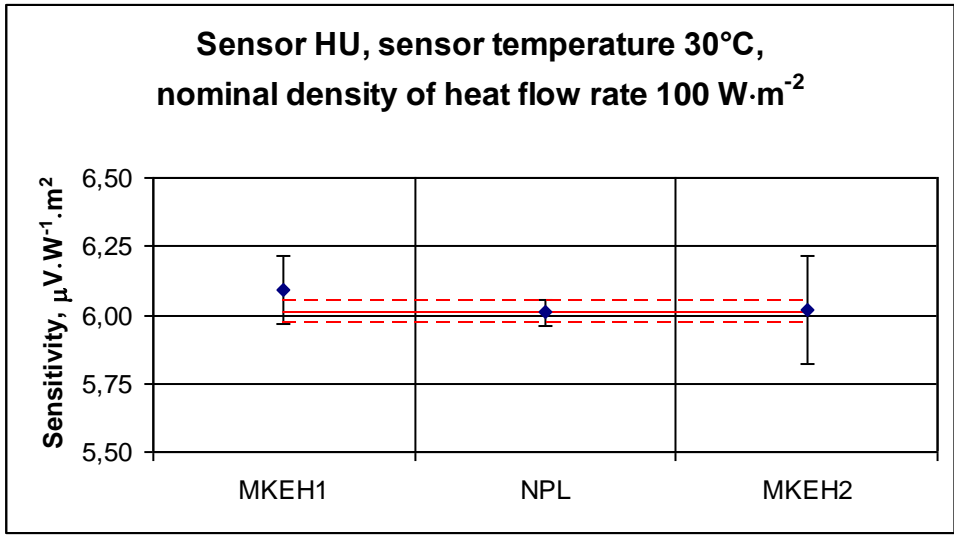


Fig. 14.3.

## 6. Evaluation of the EURAMET reference value: ERV

The ERV reference values have been evaluated according to the median. The median seem to yield the most reasonable reference value.

$$x_{ref} = median\{x_i\} \quad \sigma(x_{ref}) \cong \frac{1,9}{\sqrt{n-1}} median\left\{\left|x_{ref} - x_i\right|\right\}$$

The values of the median can be seen in Table 6.

Table 6.: ERV values

Nominal temperature [°C]	Nominal heat flux [W/m <sup>2</sup> ]	Sensor NL				Sensor HU			
		ERV value [μV/W/m <sup>2</sup> ]	Coverage factor k	Uref [μV/W/m <sup>2</sup> ]	Uref% [%] (k=2)	ERV value [μV/W/m <sup>2</sup> ]	Coverage factor k	Uref [μV/W/m <sup>2</sup> ]	Uref% [%] (k=2)
20	10	171.09	2.45	2.05	0.98	6.17	3.18	0.09	0.87
30	10	171.91	2.45	2.63	1.25	6.02	3.18	0.26	2.68
20	50	173.05	2.57	1.65	0.74	5.97	3.18	0.04	0.45
30	50	171.55	2.45	6.63	3.15	6.09	3.18	0.09	0.90
20	100	172.77	2.78	3.98	1.66	6.00	3.18	0.07	0.69
30	100	171.81	2.78	4.22	1.77	6.01	3.18	0.04	0.45

The degree of equivalence among the participants can be calculated using the following equation:

$$E_n = \frac{|S_{lab} - S_{ERV}|}{\sqrt{(U_{lab}^2 + U_{ERV}^2)}}$$

where

U - combined uncertainty of the laboratory with a coverage factor k=2

S - sensitivity of the sensor calculated from the measurement results

lab - individual results of each laboratory

ERV - reference value

The normalised deviation En is given in Table 7.

Table 7.: En values for the median

	10 [W/m <sup>2</sup> ]				50 [W/m <sup>2</sup> ]				100 [W/m <sup>2</sup> ]			
<b>Sensor NL</b>	20 [°C]		30 [°C]		20 [°C]		30 [°C]		20 [°C]		30 [°C]	
Participant	S <sub>lab-ERV</sub> [μV/W/m <sup>2</sup> ]	En	S <sub>lab-ERV</sub> [μV/W/m <sup>2</sup> ]	En	S <sub>lab-ERV</sub> [μV/W/m <sup>2</sup> ]	En	S <sub>lab-ERV</sub> [μV/W/m <sup>2</sup> ]	En	S <sub>lab-ERV</sub> [μV/W/m <sup>2</sup> ]	En	S <sub>lab-ERV</sub> [μV/W/m <sup>2</sup> ]	En
BTU	4.87	0.55	0.48	0.05	3.27	0.37	3.76	0.35	3.54	0.37	3.88	0.41
MKEH	0.18	0.04	1.05	0.24	0.18	0.05	0.00	0.00	0.00	0.00	0.00	0.00
PTB	0.17	0.04	3.01	0.63	0.67	0.16	2.60	0.34	2.59	0.46	2.53	0.44
SABS	32.97	2.29	47.27	3.61	-	-	14.18	0.81	-	-	-	-
TNO	1.79	0.38	0.91	0.18	2.55	0.56	4.85	0.61	-	-	-	-

	10 [W/m <sup>2</sup> ]				50 [W/m <sup>2</sup> ]				100 [W/m <sup>2</sup> ]			
<b>Sensor HU</b>	20 [°C]		30 [°C]		20 [°C]		30 [°C]		20 [°C]		30 [°C]	
Participant	S <sub>lab-ERV</sub> [μV/W/m <sup>2</sup> ]	En	S <sub>lab-ERV</sub> [μV/W/m <sup>2</sup> ]	En	S <sub>lab-ERV</sub> [μV/W/m <sup>2</sup> ]	En	S <sub>lab-ERV</sub> [μV/W/m <sup>2</sup> ]	En	S <sub>lab-ERV</sub> [μV/W/m <sup>2</sup> ]	En	S <sub>lab-ERV</sub> [μV/W/m <sup>2</sup> ]	En
MKEH	0.11	0.46	0.00	0.01	0.03	0.23	0.01	0.07	0.01	0.06	0.03	0.27
NPL	0.02	0.05	0.00	0.00	0.01	0.10	0.05	0.48	0.10	1.13	0.00	0.00



## 7. Conclusion

The objective of this round robin test was to improve the accuracy in the realisation of a density of heat flow rate scale up to  $100 \text{ W}\cdot\text{m}^{-2}$ , by comparing different calibration methods.

Six Institutes took part in the comparison and all the results are presented in this Report. Each one of the six partners calibrated the sensors using its individual heat source, a guarded hot plate or a heat flow apparatus. These calibration facilities used as standards assured that uniform and reliable measurements lead to comparable results. The comparison had delays caused by several reasons.

In spite of the diversity of the calibration procedures and of the characteristics of each apparatus, the measurement results are strikingly close to one another. In order to establish the uncertainty budget, the classical uncertainty contributions are extended by the instrument-and-sample-specific corrections. The characteristics of each apparatus and the detailed uncertainty evaluations are presented in the project report.

This project has shown that several Institutes are able to calibrate sensors for heat flux, and mutual deviations in the partner's results are well within their measurement uncertainties.

The importance of this comparison is given by the fact that this is the first EURAMET comparison on density of heat flow rate measurements that ever has been organised. Investigations led for laboratories to a better approach of density of heat flow rate measurements and improvements in the calibration methods and procedures. A broadening cooperation among laboratories should improve a more consistent and standardized uncertainty evaluation. The degree of equivalence, resulting from this comparison and presented in the report, could be used in order to validate the future calibration and measurement capabilities (CMCs).

## 8. References

- [1] U. Hammerschmidt: *Guarded Hot-Plate (GHP) Method: Uncertainty Assessment*, International Journal of Thermophysics, 2002, Vol. 23, No. 6.
- [2] F. van der Graaf.: *Research in Calibration and Application Errors of Heat Flux Sensors, Building Applications of Heat Flux Transducers*, ASTM STP 885, 1985.
- [3] F. van der Graaf.: *Heat Flux Sensors, Thermal Sensors*, VCH Verlagsgesellschaft, 1990.

## 9. Appendix A: Description of the measurement set-up

### 1 PTB

#### Guarded Hot-Plate (GHP) Method: Uncertainty Assessment

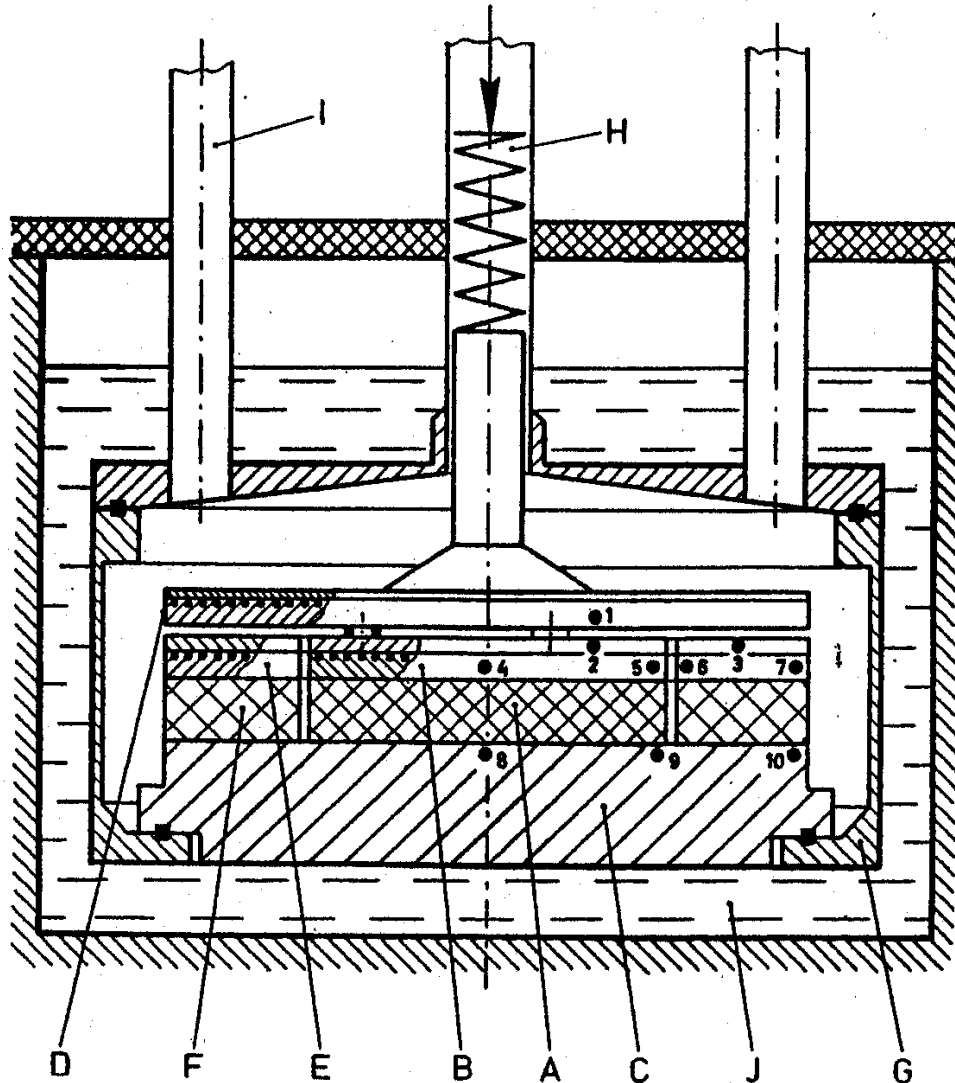


Fig. 1. Schematic of the Guarded Hot Plate Apparatus "GHP-S." A, specimen; B, hot plate; C, cold plate; D, guard plate; E, guard ring; F, edge insulation; G, casing; H, push rod; I, ducts; J, thermostated bath; 1-10, thermocouples.

The single plate GHP apparatus of PTB measures the thermal conductivity of solids between 0.01 and 6 W/m·K as a function of temperature between -80 and 200°C. The guarded hot plate is designed as a stack and accommodated in the evacuable casing (G). The cylindrical solid sample (A) with the cross-sectional area  $A$  and the thickness  $d$  is placed between the upper electrical hot plate (B) and the lower thermostated cold plate (C).

On its lateral face the sample is surrounded by edge insulation (F). The hot plate dissipates the constant electric input power  $P=U \cdot I$  as the heat flow-rate  $P$ , which on its way to the cold plate traverses the sample as homogeneously as possible. The known heat flow leads to a temperature drop across the sample which is the measure of its thermal conductivity. Two guard heaters, the guard plate (D) and the guard ring (E) that surround the hot plate are intended to establish an unidirectional and uniform heat flow of rate  $P$ . A push rod (H) which can be adjusted from outside ensures that the stack remains tightly packed without the sample being compressed. The working temperature is set by immersion of the whole apparatus in a bath thermostat (J).

The peripheral equipment consist of three constant-current sources to supply the two active guard heaters and the hot plate, a standard measuring resistor to accurately determine the current supplied to the hot plate, a twelve-channel measuring point selector switch and a digital nanovoltmeter. The instrumentation is connected to a PC, which uses PID program to bring the guarded hot plate into steady state and, subsequently collects the relevant measurement data for evaluation.

To promote good thermal contact between the specimen and the hot and cold plates, rigid specimen materials are coupled to both plates by the use of a contact medium.

## **2 SABS**

The “NL” heat flux sensor was positioned between two working standards and calibrated in a heat flow meter apparatus.

It was not possible to obtain a heat flux point  $> 30 \text{ W/m}^2$  due to instrument limitations.

### 3 MKEH

The measurements were effectuated using a RAPID k type heat flow meter apparatus. With the aid of this apparatus we are able to calibrate heat-flux sensors in the temperature range from 0 to 100°C, realising the heat flux scale in the range from 0 to 1000 W/m<sup>2</sup>, using heat flux source elaborated in our laboratory. We can also determine the thermal conductivity of different isolators from 0,01 to 2 W/m·K, in the temperature range between -30 and 200°C.

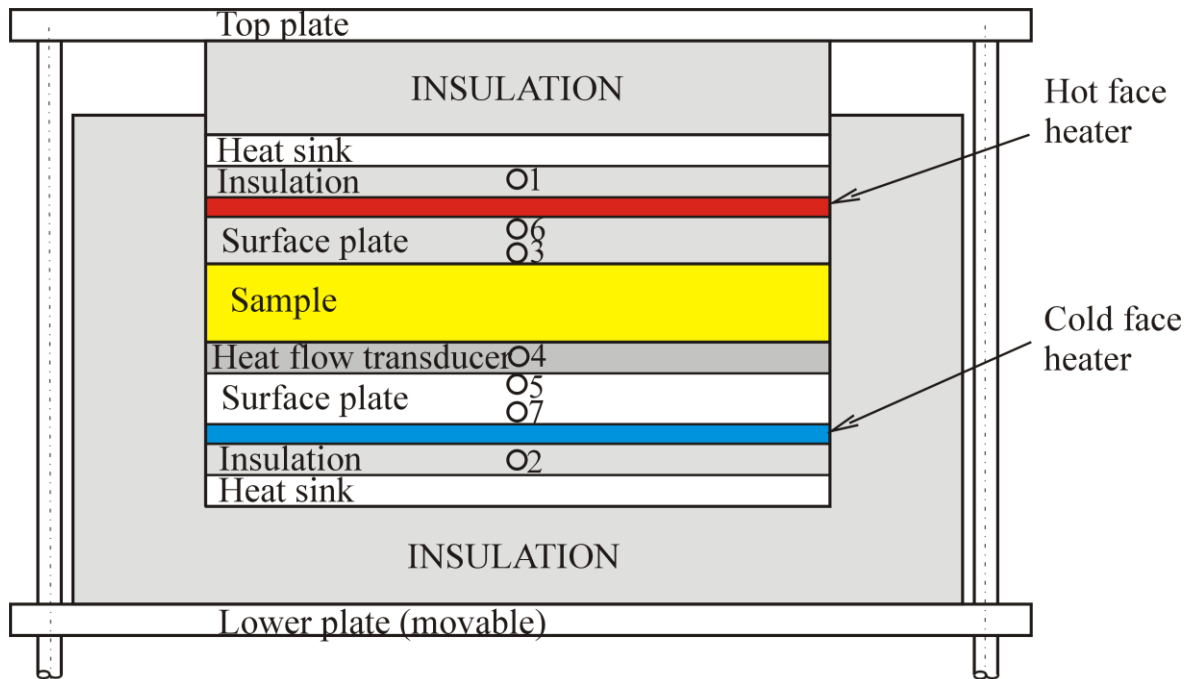


Fig. : Cross-sectional View of Rapid-k Test Section

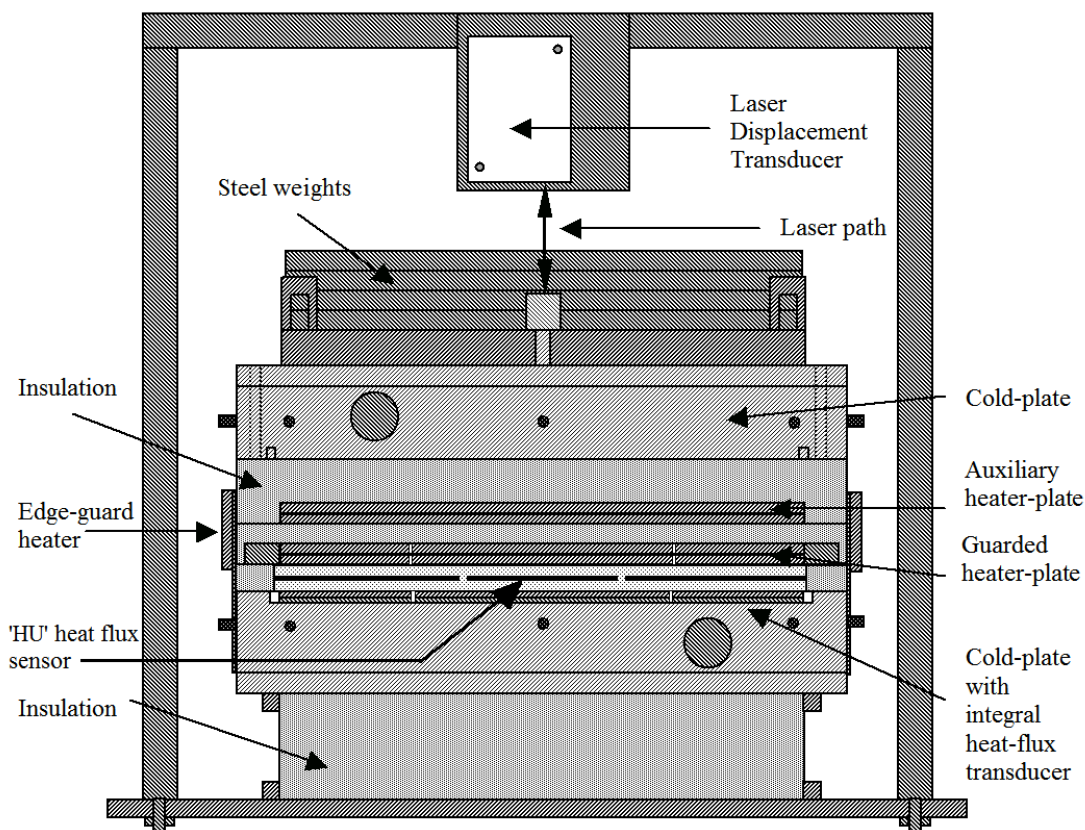
Density of heat flow rate determinations were made by placing one of the circulated heat flux sensors between two surfaces of 300 mm square area, which are maintained at known temperatures. Because of the temperature difference, heat flows through the sensor from the hot side to the cold side. The quantity of heat flowing through the heat flux sensor is measured by a heat flow transducer, a device having an output proportional to the heat flow passing through it. This transducer is placed between the heat flux sensor and the cold plate. Because some heat flows through the edges of the sensor to or from the surroundings, the heat flow measurement is made in the central 100 mm square area only.

One copper-constantan thermocouple is located in the heated upper surface adjacent to the heat flux sensor, another in the surface of the heat flow transducer below the sensor. The temperature difference across the heat flux sensor is obtained from these two thermocouples. When the handle is released, a force of approximately 200 N is exerted on the surface of the sample to assure good thermal contact. The instrumentation is connected to a PC.

## 4 NPL

The NPL measurements made for this project were undertaken using the NPL Vacuum Guarded Hot-Plate (VGHP). The VGHP is a 305 mm square, single specimen, guarded hot-plate apparatus incorporating a linear temperature gradient edge-guard.

The VGHP was designed and built at NPL and is used for measuring the thermal conductivity of a single 305 mm square specimen of material having a thermal conductivity of up to  $2 \text{ W}/(\text{m}\cdot\text{K})$  and at temperatures between  $-40^\circ\text{C}$  and  $70^\circ\text{C}$ . These thermal conductivity measurements require a steady-state heat flux through the central metering area ( $152.5 \text{ mm}$  square) of the specimen. The direction of this heat flux needs to normal the plane of the plates and its magnitude must be measured with traceability to primary national standards.



The "HU" heat flux sensor was placed between two foamed silicone rubber thermal contact sheets and then mounted in the VGHP between its heater plate and isothermal cold-plate. Three different heat fluxes were applied to the heat flux sensor at two different temperatures and the sensor's output was recorded.

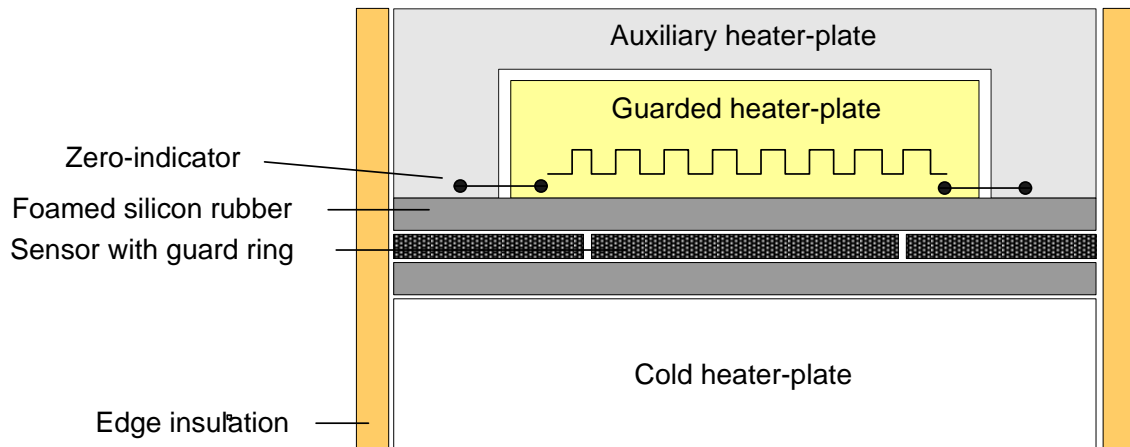
Further information on the VGHP can be found in reference:

Stacey, C., "NPL Vacuum Guarded Hot-Plate for Measuring Thermal Conductivity and Total Hemispherical Emittance of Insulation Materials," *Insulation Materials: Testing and Applications: 4th Volume, ASTM STP 1426*, A. O. Desjarlais and R. R. Zarr, Eds., American Society for Testing and Materials, West Conshohocken, PA, 2002.

Note: The information given above is correct for the time at which the measurements were made for this project. However, the VGHP has since undergone several significant upgrades to improve its performance. Current information can be obtained via the contacts given at: [www.npl.co.uk/thermalconductivity.vghp](http://www.npl.co.uk/thermalconductivity.vghp)

## 5 BTU

The instrument used at BTU is a 250 mm square, single specimen, guarded hot-plate apparatus. The temperature control of the auxiliary heater-plate and the cold heater plate is carried out by means of liquid bath thermostats with a typical stability of 10 mK. For the guarded heater-plate an electrical heater is used. The temperature difference between the auxiliary heater-plate and the guarded heater plate is measured by means of a thermopile and adjusted to “zero” (<1 mK) by a computer controlled variation of the heating power of the electrical heater. Radial heat losses are minimized by an edge insulation. The heat flux sensors were placed between foamed silicon rubber plates and surrounded by a guard ring with the same thickness and similar thermal conductivity as the heat flux sensor.



## 6 TNO

### *Heat Flux Sensors / Science / Calibration*

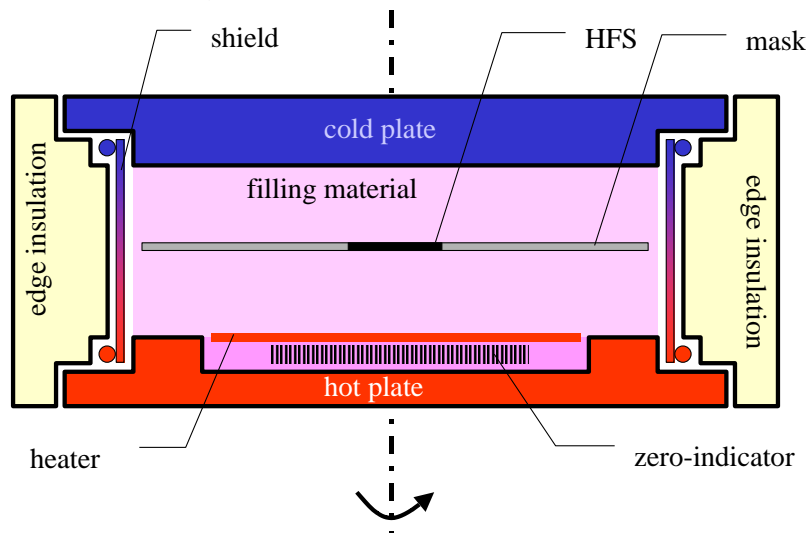
#### **Relative Calibration**

Each Heat Flux Sensor is calibrated relative to a reference Heat Flux Sensor. This Reference Sensor is of the same type as the Heat Flux Sensors which should be calibrated. The relative calibration apparatus consists of a cold and hot plate with filling material in between. The Heat Flux Sensors which should be calibrated together with the Reference Sensor are located in the middle of the filling material package. The heat flux through the apparatus is being monitored by five permanent Heat Flux Sensors. These permanent Sensors check if the heat flow is homogeneous and stable in time. If the monitored heat flux meets the requirements regarding homogeneity and stability the actual heat flux is measured and is used for calculating the calibration constant of the individual Heat Flux Sensors.



## Absolute Calibration

From each serie of Heat Flux Sensors one piece is calibrated in the ‘absolute calibration apparatus’ and is used as Reference Sensor for all other Heat Flux Sensors of the same type. A hot and cold plate create an heat flux through the filling material. An electrical heating element is located **in** the hot plate. If the temperature of the heating element is equal to the temperature of the hot plate, all heat will flow upwards (through the filling material). This is controlled by an heat flux sensor between the hot plate and the electrical heater, the so-called zero-indicator.



In this set-up all the dissipated electrical energy causes a homogeneous heat flux through the filling material. The heat flux can be calculated from the known electrical energy dissipation and the area of the heating element.

Heat losses at the edge of the set-up are eliminated by using a highly conductive metal shield. This metal shield is mounted around the filling material as a cylinder. At the upper and lower side of the shield is supplied by water channels which control respectively the cold and hot temperature. In this way a linear temperature gradient across the shield is created. This temperature gradient is equal to the gradient in the filling material. In addition the edge of the apparatus is provided by insulation. The to be calibrated Heat Flux Sensor is located in the middle of the filling material and is surrounded by a mask with the same thermal properties and thickness.

### Reference:

Graaf, F. van der, “Research in Calibration and Application Errors of Heat Flux Sensors”, published in *Building Applications of Heat Flux Transducers*, ASTM STP 885, edited by E. Bales, M. Bomberg and G.E. Courville, ASTM, 1985.

### Standards

The performance of the absolute calibration at TNO TPD is according to **ASTM C1130 (1995)**. The absolute calibration apparatus of TNO TPD meets the requirements of the International Standards **ASTM C177, DIN 52612 and ISO 8302**.

The TNO Absolute Calibration Apparatus has a few deviations from the common International Standards. These deviations have a positive effect on the result of the calibration.

- The heat losses through the edge are almost completely eliminated by the thermal shield.
- The ‘zero-indicator’ consists of thousands of thermocouples. So the sensitivity of the control parameter to equalize the temperature of the heater and the hot plate is very high.



# 10. Appendix B: Uncertainty evaluations

## 1. NPL

### EXAMPLE UNCERTAINTY BUDGET FOR THE CALIBRATION OF HEAT-FLUX TRANSDUCER 'OMH1' AT (100 W/m<sup>2</sup> & 29°C).

1. Breakdown of uncertainties associated with each measured parameter (*A to F*)
2. Uncertainty In Measurement (Equipment & Transducer)
3. Overall Measurement Uncertainty

#### UNCERTAINTIES ASSOCIATED WITH EACH MEASURED PARAMETER (*A to F*)

##### A. Heat-Flux Transducer Output

1. Resolution of dvm is 0.1 microV, for a typical signal of 500 microV (0.02%)
2. Calibration of the dvm to 0.03%
3. Calibration of voltage reference to 0.02%
4. Averaging fluctuations in output over 1000 consecutive readings gives a resolution of 1 microV, for a typical signal of 500 microV (0.2%)

<i>Source of uncertainty</i>	<i>Value +/-</i>	<i>Probability Distribution</i>	<i>Divisor</i>	<i>c( i )</i>	<i>u( i )</i>
1. Resolution of dvm / %	0.020	N	2	1	0.010
2. Calibration of dvm / %	0.030	N	2	1	0.015
3. Calibration of voltage reference / %	0.020	N	2	1	0.010
4. Averaging resolution / %	0.200	N	2	1	0.100
Combined uncertainty					0.102
<b>A. Expanded uncertainty</b>		<b>k=2</b>			<b>0.204</b>

### B. HeaterArea

The central heating area is approximately 150.5mm square and was measured using calipers in 3 positions. Some heat generated in the central area may drift into the guard/centre gap area, but as the transducer is thin and the active area is only 100mm square, this will not be significant.

The area is the mean of the two dimensions multiplied together.

1. Length measurement is able to be made to 0.1mm
2. Width measurement is able to be made to 0.1mm
3. Calibration of calipers is 0.05%
4. Resolution of calipers is 0.02 mm
5. Maximum possible additional area due to heat flux in guard/centre gap is 1 mm

<i>Source of uncertainty</i>	<i>Value +/-</i>	<i>Probability Distribution</i>	<i>Divisor</i>	<i>c( i )</i>	<i>u( i )</i>
1. Length measurement / mm	0.100	N	2	1	0.033
2. Width measurement / mm	0.100	N	2	1	0.033
3. Calibration of calipers / %	0.050	N	2	1	0.025
4. Resolution of calipers / mm	0.020	N	2	1	0.007
5. Possible additional area (gap) /mm	1.000	N	2	1	0.332
Combined uncertainty					0.336
<b>B. Expanded uncertainty</b>		<b>k=2</b>			<b>0.673</b>

### C. Measurement of Power

1. The resolution of the dvm when measuring a 1 V heater signal is 0.01 mV (0.001%)
1. Calibration of the dvm to 0.03%
3. Calibration of voltage reference to 0.02%
4. The resolution of the dvm when measuring a 100 mV signal across the SR is 0.0001 mV (0.01%)
5. Calibration of the dvm to 0.03%
6. Calibration of voltage reference to 0.02%
7. The calibration uncertainty of the Standard Resistance is 0.05%

<i>Source of uncertainty</i>	<i>Value +/-</i>	<i>Probability Distribution</i>	<i>Divisor</i>	<i>c( i )</i>	<i>u( i )</i>
1. Resolution of dvm (V) / %	0.001	N	2	1	0.001
2. Calibration of dvm (V) / %	0.030	N	2	1	0.015
3. Calibration of voltage reference (V) /%	0.020	N	2	1	0.010
4. Resolution of dvm ( I ) / %	0.010	N	2	1	0.005
5. Calibration of dvm ( I ) / %	0.030	N	2	1	0.015
6. Calibration of voltage reference ( I ) /%	0.020	N	2	1	0.010
7. Calibration of Stand. Resistor / %	0.050	N	2	1	0.025
Combined uncertainty					0.036
<b>C. Expanded uncertainty</b>		<b>k=2</b>			<b>0.072</b>

### D. Miscellaneous factors

1. Auxiliary / Meter area balance. The balance is maintained to +/- 1 micro V, which for gfb gives an uncertainty of 0.04%. (based on measurements made as part on performance checks)
2. Heat loss or gain from the specimen edges. The maximum associated uncertainty is 0.25%.

<i>Source of uncertainty</i>	<i>Value +/-</i>	<i>Probability Distribution</i>	<i>Divisor</i>	<i>c( i )</i>	<i>u( i )</i>
1. Auxiliary/meter area balance / %	0.040	N	2	1	0.020
2. Edge heat gain/loss / %	0.250	N	2	1	0.125
Combined uncertainty					0.127
<b>D. Expanded uncertainty</b>		<b>k=2</b>			<b>0.254</b>

### E. Absolute Temperature

1. The t/cs are calibrated with an uncertainty of 0.1°C, at 20°C (0.5%)
2. Linearity of least squares fit is 0.534%
3. Resolution of dvm is 0.1 microV, for a typical signal of 500 microV (0.02%)
4. Calibration of CJC/C is to 4 microV for a typical conversion of 1200 microV (0.33%)
5. Calibration of the dvm to 0.03%
6. Calibration of voltage reference to 0.02%

<i>Source of uncertainty</i>	<i>Value +/-</i>	<i>Probability Distribution</i>	<i>Divisor</i>	<i>c( i )</i>	<i>u( i )</i>
1. T/c calibration / %	0.500	N	2	1	0.250
2. Linearity of curve fit / %	0.534	N	2	1	0.267
3. Resolution of dvm / %	0.020	N	2	1	0.010
4. Calibration of CJC/C / %	0.333	N	2	1	0.167
5. Calibration of dvm / %	0.030	N	2	1	0.015
6. Calibration of voltage reference / %	0.020	N	2	1	0.010
Combined uncertainty					0.402
<b>E. Expanded uncertainty</b>		<b>k=2</b>			<b>0.805</b>

### F. Fixed Heat-Flux Offset

1. When the calibration curve is plotted, the resulting line does not pass through the origin, indicating a fixed heat-flux offset of 0.115 W/m<sup>2</sup>

<i>Source of uncertainty</i>	<i>Value +/-</i>	<i>Probability Distribution</i>	<i>Divisor</i>	<i>c( i )</i>	<i>u( i )</i>
1. Fixed heat-flux offset / W/m <sup>2</sup>	0.115	N	2	1	0.058
Combined uncertainty					0.058
<b>F. Expanded uncertainty</b>		<b>k=2</b>			<b>0.115</b>

## UNCERTAINTY IN MEASUREMENT (EQUIPMENT & TRANSDUCER)

This is split into two parts, that related to the equipment and that related to the transducer. The two must be added to give the total uncertainty for any given measurement.

### EQUIPMENT RELATED

<i>Source of uncertainty</i>	<i>Value +/-</i>	<i>Probability Distribution</i>	<i>Divisor</i>	<i>c( i )</i>	<i>u( i )</i>
A. Heat Flux Transducer Output	0.204	N	2	1	0.102
B. Heater Area	0.673	N	2	1	0.337
C. Measurement of Power	0.072	N	2	1	0.036
D. Miscellaneous Factors	0.254	N	2	1	0.127
Combined uncertainty					0.376
<b>EQUIPMENT Expanded uncertainty</b>		<b>k=2</b>			<b>0.752</b>

### TRANSDUCER RELATED

For a given specimen the effects of uncertainties in the measurement of absolute temperature, specimen density and moisture content on lambda must also be taken into account.

A 1K change in temperature produces a 0.1389  $\mu\text{V}/\text{W}/\text{m}^2$  change in a sensitivity of 6  $\mu\text{V}/\text{W}/\text{m}^2$ .

<i>Source of uncertainty</i>	<i>Value +/-</i>	<i>Probability Distribution</i>	<i>Divisor</i>	<i>c( i )</i>	<i>u( i )</i>
E. Absolute Temperature	0.805	N	2	0.466	0.188
F. Fixed Heat Flux Offset	0.115	N	2	1	0.058
Combined uncertainty					0.197
<b>TRANSDUCER Expanded uncertainty</b>		<b>k=2</b>			<b>0.394</b>

### OVERALL UNCERTAINTY IN MEASUREMENT

<i>Source of uncertainty</i>	<i>Value +/-</i>	<i>Probability Distribution</i>	<i>Divisor</i>	<i>c( i )</i>	<i>u( i )</i>
EQUIPMENT	0.752	N	2	1	0.376
TRANSDUCER	0.394	N	2	1	0.197
Combined uncertainty					0.424
<b>OVERALL Expanded uncertainty</b>		<b>k=2</b>			<b>0.848</b>

The overall measurement uncertainty is estimated to be within  $\pm 0.8\%$ , based on a standard uncertainty multiplied by a coverage factor  $k=2$ , providing a level of confidence of approximately 95%.

## 2. MKEH

$$f = f_0 + m \cdot t_a$$

$t_a$  - temperature of the cold face inside the apparatus  
 $f, f_0, m$  - factors

$$df = \frac{\partial f}{\partial f_0} df_0 + \frac{\partial f}{\partial m} dm + \frac{\partial f}{\partial t_a} dt_a$$

$$\frac{\partial f}{\partial f_0} = 1 \quad \frac{\partial f}{\partial m} = t_a \quad \frac{\partial f}{\partial t_a} = m$$

$$u(f_0) = df_0 \quad u(m) = dm \quad u(t_a) = dt_a \quad u(f) = df$$

$$u(f) = \sqrt{u(f_0)^2 + t_a^2 \cdot u(m)^2 + m^2 \cdot u(t_a)^2}$$

$$f_0 = 31.38 \text{ [W / m}^2 \cdot \text{mV]} \quad u(f_0) = 0.01$$

$$m = -0.019 \text{ [W / m}^2 \cdot \text{mV} \cdot \text{°C]} \quad u(m) = 0.001$$

$$u(t_a)^2 = u(t_a)_C^2 + u(t_a)_S^2$$

$$u(t_a)_C = 0.1^\circ\text{C}$$

$$u(t_a)_S = 0.01^\circ\text{C} \quad (t_a = 20^\circ\text{C})$$

$$u(t_a)_S = 0.03^\circ\text{C} \quad (t_a = 30^\circ\text{C})$$

$$q = f \cdot V_h$$

$q$  - density of heat flow rate  
 $V_h$  - voltage of the standard heat flux sensor inside the apparatus

$$dq = \frac{\partial q}{\partial f} df + \frac{\partial q}{\partial V_h} dV_h$$

$$\frac{\partial q}{\partial f} = V_h \quad \frac{\partial q}{\partial V_h} = f$$

$$u(f) = df \quad u(V_h) = dV_h \quad u(q) = dq$$

$$u(q) = \sqrt{V_h^2 \cdot u(f)^2 + f^2 \cdot u(V_h)^2}$$

$$u(V_h) = 0.01 \cdot V_h$$

$$S = \frac{V_s}{q}$$

$S$  - sensitivity of the heat flux sensor  
 $V_s$  - voltage of the sensor output

$$dS = \frac{\partial S}{\partial V_s} dV_s + \frac{\partial S}{\partial q} dq$$

$$\frac{\partial S}{\partial V_s} = \frac{1}{q} \quad \frac{\partial S}{\partial q} = -\frac{V_s}{q^2}$$

$$u(V_s) = dV_s \quad u(q) = dq \quad u(S) = dS$$

$$u(S) = \sqrt{\frac{1}{q^2} \cdot u(V_s)^2 + \frac{V_s^2}{q^4} \cdot u(q)^2}$$

$$u(V_s)^2 = u(V_s)_R^2 + u(V_s)_C^2 + u(V_s)_{FL}^2$$

For sensor “NL”:  $u(V_s)_R = 0.3\mu V$   $u(V_s)_C = 2\mu V$

$u(V_s)_{FL} = 3\mu V$

For sensor “HU”:  $u(V_s)_R = 0.3\mu V$   $u(V_s)_C = 1\mu V$

$u(V_s)_{FL} = 0.3\mu V$

### Sensor “NL”

Nominal temp. [°C]	Nominal heat flux [W/m <sup>2</sup> ]	t <sub>a</sub> [°C]	u(t <sub>a</sub> ) [°C]	f = f <sub>0</sub> + m · t [W/m <sup>2</sup> · mV]	u(f) [W/m <sup>2</sup> · mV]	V <sub>h</sub> [mV]	u(V <sub>h</sub> ) [mV]	q = f · V <sub>h</sub> [W/m <sup>2</sup> ]	u(q) [W/m <sup>2</sup> ]
20	10	19.24	0.1005	31.014	0.02177	0.316148	0.003161	9.805	0.09829
30	10	30.24	0.1044	30.805	0.03191	0.328973	0.003290	10.134	0.10188
20	50	18.54	0.1005	31.028	0.02115	1.739042	0.017390	53.959	0.54084
30	50	28.29	0.1044	30.842	0.03007	1.597205	0.015972	49.261	0.49495
20	100	17.04	0.1005	31.056	0.01985	3.333333	0.033333	103.52	1.03731
30	100	25.48	0.1044	30.896	0.02744	3.258027	0.032580	100.66	1.01056

Nominal temp. [°C]	Nominal heat flux [W/m <sup>2</sup> ]	V <sub>s</sub> [μV]	u(V <sub>s</sub> ) [μV]	S = $\frac{V_s}{q}$ [μV · m <sup>2</sup> /W]	u(S) [μV · m <sup>2</sup> /W]	U(S) k=2 [μV · m <sup>2</sup> /W]	U(S) [%]
20	10	1679.20	3.61801	171.26	1.7560	3.5120	2.0507
30	10	1758.54	3.61801	173.53	1.7807	3.5615	2.0524
20	50	9357.26	3.61801	173.41	1.7395	3.4789	2.0062
30	50	8426.26	3.61801	171.19	1.7202	3.4404	2.0097
20	100	17887.23	3.61801	172.79	1.7318	3.4636	2.0045
30	100	17270.53	3.61801	171.57	1.7229	3.4457	2.0083



## Sensor “HU”

Nominal temp. [°C]	Nominal heat flux [W/m <sup>2</sup> ]	$t_a$ [°C]	$u(t_a)$ [°C]	$f = f_0 + m \cdot t$ [W/m <sup>2</sup> · mV]	$u(f)$ [W/m <sup>2</sup> · mV]	$V_h$ [mV]	$u(V_h)$ [mV]	$q = f \cdot V_h$ [W/m <sup>2</sup> ]	$u(q)$ [W/m <sup>2</sup> ]
20	10	18.96	0.1005	31.020	0.02152	0.348259	0.003483	10.803	0.10829
30	10	29.15	0.1044	30.826	0.03088	0.426945	0.004269	13.161	0.13227
20	50	17.39	0.1005	31.050	0.02015	1.631143	0.016311	50.647	0.50754
30	50	26.93	0.1044	30.868	0.02880	1.681515	0.016815	51.905	0.52130
20	100	15.02	0.1005	31.095	0.01815	3.229555	0.032296	100.42	1.00594
30	100	24.74	0.1044	30.910	0.02676	3.238078	0.032381	100.09	1.00463

Nominal temp. [°C]	Nominal heat flux [W/m <sup>2</sup> ]	$V_s$ [μV]	$u(V_s)$ [μV]	$S = \frac{V_s}{q}$ [μV · m <sup>2</sup> /W]	$u(S)$ [μV · m <sup>2</sup> /W]	$U(S)$ k=2 [μV · m <sup>2</sup> /W]	$U(S)$ [%]
20	10	66.66	1.08628	6.171	0.1181	0.2361	3.8261
30	10	78.41	1.08628	5.958	0.1020	0.2039	3.4229
20	50	302.13	1.08628	5.965	0.0635	0.1270	2.1294
30	50	317.23	1.08628	6.112	0.0649	0.1297	2.1221
20	100	604.34	1.08628	6.018	0.0612	0.1225	2.0354
30	100	600.77	1.08628	6.002	0.0612	0.1224	2.0399

### 3. SABS

1 Mar. '02 8:19

FAX

P. 3

<b>UNCERTAINTY BUDGET</b>									
References: ISO/IEC 17025-4 Guide to the Expression of Uncertainty in Measurements - 1993 (BIPM, IEC, IFCC, ISO, IUPAC, IUPAP, OIML), MS 3083, EAL R2									
Title: Euromet Interlaboratory Comparison Pr 426 Range: 10 W/m <sup>2</sup> Metrologist: CG Kros									
Title: STD + ACC + REP									
Symbol	Source of Uncertainty	Value [%]	Probability Distribution	Divisor factor	Sensitivity Coefficient	Uncertainty Contribution (% )	Reliability %	Degree of Freedom	REMARKS
STD	Traceability - cal of instrument	8.96	N	2		4.48	100	infinite	See note 1
ACC	Instrument accuracy	5	R	2		2.50	100	infinite	
REP	Repeatability of	0.4	N	1		0.40		5.00	
						Combined Uncertainty Normal		5.15	
						Expanded Uncertainty Normal(k=2)		10.29	
						V eff		1.37E+05	
						t 95.45(v)		2.00	

Instrument calibrated with SRM.

## UNCERTAINTY BUDGET

References: ISO/IEC 17025:2005 / Guide to the Expression of Uncertainty in Measurements (GUM) / JCSS Working Group 1 / JCSS WG 1 / JCSS WG 1 / JCSS WG 1 / JCSS WG 1

Description : Euromet Interlaboratory Comparison Pr. 426

Range : 50 W/m<sup>2</sup>

Metrologist : CG Kros

Formula:  $STD + ACC + RES$


Type	Symbol	Source of Uncertainty	Value (%)	Probability Distribution	Divisor factor	Sensitivity Coefficient	Uncertainty Contribution (%)	Reliability (%)	Degree of Freedom	REMARKS									
B	STD	Traceability - cal of instrument	8.96	N	2		4.48	100	infinite	See note 1									
B	ACC	Instrument accuracy	5	R	2		2.50	100	infinite										
A	REP	Repeatability of	0.03	N	1		0.03		5.00										
<table border="1" style="width: 100%; border-collapse: collapse;"> <tr> <td style="width: 50%;">Combined Uncertainty</td> <td>Normal</td> <td>5.13</td> <td>V eff</td> <td>4.28E+09</td> </tr> <tr> <td>Expanded Uncertainty</td> <td>Normal(k=2)</td> <td>10.26</td> <td>95.45%(v)</td> <td>2.00</td> </tr> </table>										Combined Uncertainty	Normal	5.13	V eff	4.28E+09	Expanded Uncertainty	Normal(k=2)	10.26	95.45%(v)	2.00
Combined Uncertainty	Normal	5.13	V eff	4.28E+09															
Expanded Uncertainty	Normal(k=2)	10.26	95.45%(v)	2.00															

Note 1 : Instrument calibrated with SRM.

## 4. BTU

Kalibrierung eines Wärmestromdichtesensors (BTU)		
<b>Kalibrierung eines Wärmestromdichtesensors (BTU)</b>		
<b>Modellgleichung:</b>		
$c_{\text{Sensor}} = (P_0 - P_v - P_{\text{Spalt}} - P_z - P_{\text{Rand}}) / (U_{\text{Sensor}} \cdot A);$		
$A = \pi \cdot (d_i \cdot (1 + \alpha \cdot (T_m - T_0)))^2 / 4;$		
$P_0 = U_H^2 / R_H;$		
$P_v = c_1 \cdot \Delta U_{\text{tp}};$		
$P_{\text{Spalt}} = (\lambda_{\text{Spalt}} \cdot A_{\text{Spalt}} \cdot \Delta T) / (2 \cdot d);$		
<b>Liste der Größen:</b>		
Größe	Einheit	Definition
$c_{\text{Sensor}}$	W / (mV*m <sup>2</sup> )	Empfindlichkeit (Kalibrierwert) des Wärmestromdichtesensors
$P_0$	W	Heizleistung
$P_v$	W	Ringverstimmungskorrektion
$P_{\text{Spalt}}$	W	Spaltkorrektion
$P_z$	W	Zuleitungskorrektion
$P_{\text{Rand}}$	W	Randverluste (Bode)
$U_{\text{Sensor}}$	mV	Thermospannung des Sensors
$A$	m <sup>2</sup>	Fläche der Heizplatte
$\pi$		
$d_i$	m	Durchmesser der Heizplatte
$\alpha$	K <sup>-1</sup>	thermischer Ausdehnungskoeffizient des Heizplattenmaterials
$T_m$	°C	Heizplattentemperatur
$T_0$	°C	23,0 °C
$U_H$	V	Heizspannung
$R_H$	Ohm	Heizwiderstand
$c_1$	W / μV	s. Ringverstimmungskorrektion
$\Delta U_{\text{tp}}$	μV	Thermospannung der Thermosäule zur Differenztemperaturmessung zwischen Heizplatte und Heizring
$\lambda_{\text{Spalt}}$	W / (m*K)	Wärmeleitfähigkeit des Spaltmaterials
$A_{\text{Spalt}}$	m <sup>2</sup>	Spaltfläche
$\Delta T$	K	Temperaturdifferenz (Spaltkorrektion)
$d$	m	"Probendicke" (Spaltkorrektion)
$c_{\text{Sensor}}$ :	Ergebnis	
$P_0$ :	Zwischenergebnis	
Datum: 12.10.2000	Datei: EUROMET426	Seite 1 von 5

Kalibrierung eines Wärmestromdichtesensors (BTU)		
<b>P<sub>v</sub>:</b>	Zwischenergebnis	
<b>P<sub>Spalt</sub>:</b>	Zwischenergebnis	
<b>P<sub>Z</sub>:</b>	Typ B Rechteckverteilung Wert: 0 W Halbbreite der Grenzen: 0.039 W	
<b>P<sub>Rand</sub>:</b>	Typ B Normalverteilung Wert: 0 W Erweiterte Messunsicherheit: $6.5 \cdot 10^{-4}$ W Erweiterungsfaktor: 2	
<b>U<sub>Sensor</sub>:</b>	Typ B Rechteckverteilung Wert: 18.1487 mV Halbbreite der Grenzen: 0.01 mV	
<b>A:</b>	Zwischenergebnis	
<b><math>\pi</math>:</b>	Konstante Wert: 3.14159265358979323846	
<b>d<sub>i</sub>:</b>	Typ B Normalverteilung Wert: 0.1156 m Erweiterte Messunsicherheit: 0.0007 m Erweiterungsfaktor: 1	
<b><math>\alpha</math>:</b>	Typ B Rechteckverteilung Wert: $2.4 \cdot 10^{-5}$ K <sup>-1</sup> Halbbreite der Grenzen: $2 \cdot 10^{-6}$ K <sup>-1</sup>	
<b>T<sub>m</sub>:</b>	Typ B Rechteckverteilung Wert: 29.0 °C Halbbreite der Grenzen: 0.3 °C	
<b>T<sub>0</sub>:</b>	Typ B Rechteckverteilung Wert: 23 °C Halbbreite der Grenzen: 0.5 °C	
<b>U<sub>H</sub>:</b>	Typ B Rechteckverteilung Wert: 8.73037 V Halbbreite der Grenzen: 0.005 V	
<b>R<sub>H</sub>:</b>	Typ B Normalverteilung Wert: 69.918 Ohm Erweiterte Messunsicherheit: 0.093 Ohm Erweiterungsfaktor: 1	
Datum: 12.10.2000	Datei: EUROMET426	Seite 2 von 5

Kalibrierung eines Wärmestromdichtesensors (BTU)		
<b>c<sub>1</sub>:</b>	Typ B Rechteckverteilung Wert: $4.9 \cdot 10^{-4} \text{ W} / \mu\text{V}$ Halbbreite der Grenzen: $5 \cdot 10^{-5} \text{ W} / \mu\text{V}$	
<b><math>\Delta U_{tp}</math>:</b>	Typ B Rechteckverteilung Wert: $0.4 \mu\text{V}$ Halbbreite der Grenzen: $20 \mu\text{V}$	
<b><math>\lambda_{Spalt}</math>:</b>	Typ B Normalverteilung Wert: $0.062 \text{ W} / (\text{m} \cdot \text{K})$ Erweiterte Messunsicherheit: $3.1 \cdot 10^{-3} \text{ W} / (\text{m} \cdot \text{K})$ Erweiterungsfaktor: 2	
<b>A<sub>Spalt</sub>:</b>	Typ B Normalverteilung Wert: $1.81 \cdot 10^{-4} \text{ m}^2$ Erweiterte Messunsicherheit: $3.6 \cdot 10^{-5} \text{ m}^2$ Erweiterungsfaktor: 2	
<b><math>\Delta T</math>:</b>	Typ B Rechteckverteilung Wert: $12.0 \text{ K}$ Halbbreite der Grenzen: $0.1 \text{ K}$	
<b>d:</b>	Typ B Rechteckverteilung Wert: $6.7 \cdot 10^{-3} \text{ m}$ Halbbreite der Grenzen: $0.1 \cdot 10^{-3} \text{ m}$	
Datum: 12.10.2000	Datei: EUROMET426	Seite 3 von 5

**Messunsicherheits-Budget:**

Größe	Wert	Std.-Mess-unsicherheit	Freiheits-grad	Sensitivitäts-koeffizient	Unsicher-heitsbeitrag
$P_0$	1.09013 W	$1.62 \cdot 10^{-3}$ W			
$P_V$	$200 \cdot 10^{-6}$ W	$5.66 \cdot 10^{-3}$ W			
$P_{\text{Spalt}}$	0.01005 W	$1.04 \cdot 10^{-3}$ W			
$P_Z$	0.0 W	0.0225 W	unendlich	-5.2	-0.12 W / (mV*m <sup>2</sup> )
$P_{\text{Rand}}$	0.0 W	$325 \cdot 10^{-6}$ W	50	-5.2	$-1.7 \cdot 10^{-3}$ W / (mV*m <sup>2</sup> )
$U_{\text{Sensor}}$	18.14870 mV	$5.77 \cdot 10^{-3}$ mV	unendlich	-0.31	$-1.8 \cdot 10^{-3}$ W / (mV*m <sup>2</sup> )
A	0.010499 m <sup>2</sup>	$127 \cdot 10^{-6}$ m <sup>2</sup>			
$\pi$	3.1415926535898				
$d_i$	0.115600 m	$700 \cdot 10^{-6}$ m	50	-98	-0.069 W / (mV*m <sup>2</sup> )
$\alpha$	$24.00 \cdot 10^{-6}$ K <sup>-1</sup>	$1.15 \cdot 10^{-6}$ K <sup>-1</sup>	unendlich	-68	$-79 \cdot 10^{-6}$ W / (mV*m <sup>2</sup> )
$T_m$	29.000 °C	0.173 °C	unendlich	$-270 \cdot 10^{-6}$	$-47 \cdot 10^{-6}$ W / (mV*m <sup>2</sup> )
$T_0$	23.000 °C	0.289 °C	unendlich	$270 \cdot 10^{-6}$	$79 \cdot 10^{-6}$ W / (mV*m <sup>2</sup> )
$U_H$	8.73037 V	$2.89 \cdot 10^{-3}$ V	unendlich	1.3	$3.8 \cdot 10^{-3}$ W / (mV*m <sup>2</sup> )
$R_H$	69.9180 Ohm	0.0930 Ohm	50	-0.082	$-7.6 \cdot 10^{-3}$ W / (mV*m <sup>2</sup> )
$c_1$	$490.0 \cdot 10^{-6}$ W / $\mu$ V	$28.9 \cdot 10^{-6}$ W / $\mu$ V	unendlich	-2.1	$-61 \cdot 10^{-6}$ W / (mV*m <sup>2</sup> )
$\Delta U_{\text{tp}}$	0.4 $\mu$ V	11.5 $\mu$ V	unendlich	$-2.6 \cdot 10^{-3}$	-0.030 W / (mV*m <sup>2</sup> )
$\lambda_{\text{Spalt}}$	0.06200 W / (m*K)	$1.55 \cdot 10^{-3}$ W / (m*K)	50	-0.85	$-1.3 \cdot 10^{-3}$ W / (mV*m <sup>2</sup> )
$A_{\text{Spalt}}$	$181.0 \cdot 10^{-6}$ m <sup>2</sup>	$18.0 \cdot 10^{-6}$ m <sup>2</sup>	50	-290	$-5.2 \cdot 10^{-3}$ W / (mV*m <sup>2</sup> )
$\Delta T$	12.0000 K	0.0577 K	unendlich	$-4.4 \cdot 10^{-3}$	$-250 \cdot 10^{-6}$ W / (mV*m <sup>2</sup> )
d	$6.7000 \cdot 10^{-3}$ m	$57.7 \cdot 10^{-6}$ m	unendlich	7.9	$450 \cdot 10^{-6}$ W / (mV*m <sup>2</sup> )
$c_{\text{Sensor}}$	5.67 W / (mV*m <sup>2</sup> )	0.140 W / (mV*m <sup>2</sup> )	870		

**Ergebnis:** Messgröße:  $c_{\text{Sensor}}$   
Wert:  $5.67 \text{ W} / (\text{mV} \cdot \text{m}^2)$   
Erweiterte Messunsicherheit:  $\pm 0.28 \text{ W} / (\text{mV} \cdot \text{m}^2)$   
Erweiterungsfaktor: 2.0  
Überdeckung: t-Tabelle 95%



Brandenburgische  
Technische Universität Cottbus  
Lehrstuhl für Angewandte Physik  
Prof. Dr. H. Rogäß  
Postfach 10 13 44  
03013 Cottbus



1. Thermal conductivity in  $W \cdot m^{-1} \cdot K^{-1}$ : 1.13
2. Working temperature in  $^{\circ}C$ : 20
3. Heat flow in  $W$ : 8.9
4. Temperature difference in  $K$ : 10
5. Sample thickness in  $mm$ : 10
6. Temperature gradient in  $K \cdot m^{-1}$ : 1000
7. Sample diameter in  $mm$ : 100
8. Sample area in  $mm^2$ : 7853.98

5. STANDARD UNCERTAINTY

5.1. Variances

The combined standard uncertainty  $u_c(y)$  is defined by Eq. (1). In the mathematical model, Eq. (21), all input quantities are assumed uncorrelated. Thus, the following equations are valid:

$$u_c^2(\lambda) = c_P^2 u^2(P) + c_A^2 u^2(A) + c_{AT}^2 u^2(AT) + c_d^2 u^2(d) \quad (22)$$

with:

$$c_P^2 u^2(P) = c_{P0}^2 u^2(P_0) + c_{Px}^2 u^2(P_x) + c_{FPV}^2 u^2(P_V) \quad (23)$$

$$c_A^2 u^2(A) = c_{A0}^2 u^2(r_0) + c_{A\alpha}^2 u^2(\alpha) + c_{T0}^2 u^2(T_0) + c_{Tm}^2 u^2(T_m) \quad (24)$$

$$c_d^2 u^2(d) = c_{d0}^2 u^2(d_0) + c_{d\alpha}^2 u^2(\alpha) + c_{T0}^2 u^2(T_0) + c_{Tm}^2 u^2(T_m) \quad (25)$$

$$c_{AT}^2 u^2(AT) = c_{AT0}^2 u^2(AT_0) + c_{ATb}^2 u^2(AT_b) + c_{ATc}^2 u^2(AT_c) \quad (26)$$

where:

$$c_{P0} = \frac{\partial \lambda(T_m)}{\partial P_0} = \frac{1}{N_1} \frac{Z_2}{N_2} \quad c_{AT0} = \frac{\partial \lambda(T_m)}{\partial AT_0} = \frac{Z_1}{N_1} \frac{Z_2}{N_2}$$

$$c_{Px} = \frac{\partial \lambda(T_m)}{\partial P_x} = \frac{1}{N_1} \frac{Z_2}{N_2} \quad c_{ATb} = \frac{\partial \lambda(T_m)}{\partial AT_b} = \frac{Z_1}{N_1} \frac{Z_2}{N_2}$$

$$c_{FPV} = \frac{\partial \lambda(T_m)}{\partial \Sigma P_{Vi}} = \frac{1}{N_1} \frac{Z_2}{N_2} \quad c_{ATc} = \frac{\partial \lambda(T_m)}{\partial AT_c} = \frac{Z_1}{N_1} \frac{Z_2}{N_2}$$

$$c_{d0} = \frac{\partial \lambda(T_m)}{\partial d_0} = \frac{2Z_1}{N_1} \frac{Z_2}{r_0 N_2} \quad c_{d\alpha} = \frac{\partial \lambda(T_m)}{\partial d_{\alpha}} = \frac{Z_1}{N_1} \frac{1}{N_2}$$

**Determination:** Experimental estimate of the radiative exchange by variation of the specimen thickness as well as of the temperature difference across the sample. As an alternative, a theoretical approximation can be calculated with the aid of infrared absorption spectra.

4.2.2. Model of the Guarded Hot Plate

In the real model of the single guarded hot plate, Eq. (21), all apparatus-specific corrections mentioned above have been taken into account. The following is obtained:

$$\lambda(T_m) = \frac{P_0 - P_x - \sum_{i=1}^3 P_{Vi}}{\pi [r_0 (1 + \alpha(T_0 - T_m))]^2 AT_0 - (AT_b + AT_c)} \quad (21)$$

$$\lambda(T_m) = \frac{P_0 - P_x - \sum_{i=1}^3 P_{Vi}}{\pi r_0^2 [1 + \alpha(T_0 - T_m)] AT_0 - AT_b - AT_c} \frac{d_0}{d_0}$$

$$= \frac{Z_1 Z_2}{N_1 N_2}$$

In these relations, the thermal expansion coefficient  $\alpha$ , its reference temperature  $T_0$  ( $=23^{\circ}C$ ), and the mean temperature  $T_m$  are considered to be constant.

4.2.3. Validity of the Model

The mathematical model, Eq. (21), valid for the following ranges of thermal and mechanical properties:

1. Range of measurement in  $W \cdot m^{-1} \cdot K^{-1}$ :  $0.01 < \lambda < 6$
2. Mean temperature in  $^{\circ}C$ :  $-75 < T < 195$
3. Heat flow in  $W$ :  $0 < P_0 < 120$
4. Temperature difference in  $K$ :  $5 < AT < 20$
5. Sample thickness in  $mm$ :  $5 < d < 25$
6. Temperature gradient in  $K \cdot m^{-1}$ :  $\leq 3 \times 10^3$
7. Sample diameter in  $mm$ : 100
8. Sample area in  $mm^2$ : 7853.98

The subsequent evaluation of the standard uncertainty is assessed with the following values as obtained from a measurement on the standard reference CRM 039 (Pyrex 7740) which has been taken as a concrete example. The Pyrex 7740 glass was manufactured by Corning France.

### 5.1.1. Geometry of Sample

*Type A:* The cylindrical sample should be plane-parallel and sharp-edged. The unavoidable deviations from plane parallelism are compensated for with silicone oil when coupling to the hot and cold plates takes place. The cross-sectional area of the sample,  $A = \pi r^2$  (theoretical size: 7853.98 mm<sup>2</sup>), and its thickness  $d$  (theoretical size: 10 mm) are determined from a series of  $N = 15$  observations. The uncertainties and variances according to Eq. (4) in relative terms are

$$u(\bar{A}) = 2(0.05\%) = 0.1\%$$

and in absolute terms

$$u(\bar{A}) = 7.85 \times 10^{-6} \text{ m}$$

$$u^2(\bar{A}) = 6.2 \times 10^{-11} \text{ m}^2$$

and

$$u(\bar{d}) = 0.05\%$$

$$u(\bar{d}) = 5 \times 10^{-6} \text{ m}$$

$$u^2(\bar{d}) = 2.5 \times 10^{-11} \text{ m}^2$$

respectively.

*Type B:* An estimate of  $u(d)$  according to Eq. (6) and the statement "exact to 1/100 (mm)" furnishes:

$$u^2(d) = \frac{1}{12}(a_+ - a_-)^2 = \frac{1}{12}(10.01 \times 10^{-3} - 9.99 \times 10^{-3})^2 \text{ m}^2 = 3.33 \times 10^{-11} \text{ m}^2$$

$$u(d) = 5.8 \times 10^{-6} \text{ m}$$

At a working temperature  $T_A = 20^\circ\text{C}$ , the thermal expansion of the Pyrex sample need not be taken into consideration.

### 5.1.2. Temperature Differences

*Type A:* The observed mean values from 15 measurements of each of the ten individual temperatures, measured as thermoelectric voltage  $U_{Th}$  (cf., Fig. 1) and converted into temperatures  $T$  in accordance with the individual calibration tables, show a maximum standard deviation of 40 mK. The uncertainty  $u(\Delta\bar{T})$  for the required temperature differences thus is:

$$u(\Delta\bar{T}) = \sqrt{(40 \times 10^{-3})^2 + (40 \times 10^{-3})^2} \text{ K} = 5.7 \times 10^{-2} \text{ K}$$

and the variance

$$u^2(\Delta\bar{T}) = 3.2 \times 10^{-3} \text{ K}^2.$$

Due to the great efforts which would have to be made, a description of the alternative determination of  $u(\Delta\bar{T})$  by the *type B* procedure is not carried out.

### 5.1.3. Heat flow

*Type A:* The (gross) heat flow is determined from the electric input power  $P = UI$  of the hot plate. For this purpose, the voltage drop  $U$  across the heater is directly measured and the current is determined indirectly from the voltage drop  $U_R$  across a calibrated four-pole standard resistor  $R = 1 \Omega$ . Thus  $P = UU_R/R$  holds. Repeat observations show that the variance of the power is

$$u^2(\bar{P}) = 5.1 \times 10^{-8} \text{ W}^2.$$

*Type B:* For the DVM, the manufacturer specifies a resolution of 10  $\mu\text{V}$  and maximum permissible errors (accuracy) of  $\pm 10$  ppm of the voltage reading +4 ppm for the ranges of measurement 3 and 30 V, respectively. These data have been verified by in-house calibration. For the measured value  $U = 20$  V, the resulting maximum permissible errors are  $3.2 \times 10^{-4}$  V and for the measured value  $U_R = 0.5$  V, according to the maximum permissible errors,  $1.7 \times 10^{-5}$  V. With Eq. (6) the following two variances follow:

$$u^2(U) = 3.4 \times 10^{-8} \text{ V}^2$$

and

$$u^2(U_R) = 9.6 \times 10^{-11} \text{ V}^2.$$

The calibration certificate for the standard resistor  $R = 1 \Omega$  confirms an uncertainty  $u(R) = 5 \times 10^{-6} \Omega$  so that the variance is given by

$$u^2(R) = 2.5 \times 10^{-11} \Omega^2.$$

Finally, the following relation is obtained for the variance of the quantity  $P$  using Eq. (1), the error propagation law:

$$u^2(P) = \left(\frac{U_R}{R}\right)^2 u^2(U) + \left(\frac{U}{R}\right)^2 u^2(U_R) + \left(\frac{UU_R}{R^2}\right)^2 u^2(R) = 4.7 \times 10^{-8} \text{ W}^2,$$

which still agrees quite well with the above-mentioned value.

### 5.1.4. Heat Flow Correction Factors

*Type A:* The values of the coefficients  $C_1$  and  $C_5$  from Eqs. (10) and (11) were determined by thermal mismatching (cf., Ref. 8); their individual uncertainties may be estimated at 5% at most. This relatively large value does not, however, exert such a substantial influence on the overall uncertainty budget; experience has shown that the correction factors  $P_{v1}$  and  $P_{v2}$  amount only to about 0.1% of  $P_0$ . The relative uncertainty of  $P_{v3}$  is 20% at most. Since  $P_{v3}/P_0 \approx 0.1\%$  is valid, the influence on the uncertainty of the gross heat flow remains approximately 0.02%. Repeat observations furnish the following variances:

$$u^2(\bar{P}_{v1}) = 8.5 \times 10^{-7} \text{ W}^2$$

$$u^2(\bar{P}_{v2}) = 8.5 \times 10^{-7} \text{ W}^2$$

$$u^2(\bar{P}_{v3}) = 8.5 \times 10^{-7} \text{ W}^2$$

This applies similarly to the quantity  $P_x$ . Here, the uncertainty of 0.08% is obtained from the series of measurements. The resulting variance is

$$u^2(\bar{P}_x) = 1.5 \times 10^{-7} \text{ W}^2$$

The stray heat flow  $P_{v4}$  from the edge heat loss error (gap) for the guard plate can be neglected because the working temperature is 20°C. The stray heat flow  $P_{v5}$  from the heat loss error at the sample's lateral surface may also be neglected, as the thermal conductivity of the Pyrex sample under test is still high compared with the thermal conductivity of the protective ring (Fig. 1: element (F)).

*Type B:* A determination of the variances of the stray heat flows by the *type B* procedure is most complicated as the mathematical relations are indeterminate.

### 5.2. Specimen-Specific Corrections

The temperature jump at the front faces of the specimen in most cases cannot be adequately described mathematically. The influence must be estimated for each individual case. For the measurement on Pyrex glass, this effect may certainly be neglected. The second sample-specific effect mentioned above, the radiative transport in the sample, need not be corrected either. Infrared absorption spectra on Pyrex measured at PTB do not show significant transference in the working temperature range of the guarded hot plate.

### 5.3. Covariances

To determine the electric input power,  $P = UU_R/R$ , the voltages  $U$  and  $U_R$  are measured using the same voltmeter. Thus, the associated uncertainty contributions are, strictly speaking, correlated. This effect leads to an increase in the uncertainty because the product of both voltages appears. However, compared with the uncertainty in determining the rate of heat flow (cf., Section 5.1.3) the contribution due to correlation is negligible.

### 5.4. Uncertainty Budget

Table III contains all data important for the uncertainty analysis such as input quantities, their estimated values as well as the associated sensitivity coefficients and the variances determined.

The absolute standard uncertainty to be assigned to the measurement result on Pyrex at 20°C (cf. Section 4.2.3.) reads:

$$u(\lambda) = \sqrt{1.21 \times 10^{-4} \text{ W}^2 \cdot \text{m}^{-2} \cdot \text{K}^{-2}} = 0.011 \text{ W} \cdot \text{m}^{-1} \cdot \text{K}^{-1}$$

Just as here, a normal distribution can generally be assigned to the measurand. The result given then is valid for a coverage probability of 68.3%. With this probability the measured value lies in the confidence interval  $\pm u(\lambda)$ . According to the resolution adopted by the EA (European Cooperation for Accreditation), a so-called expanded uncertainty of measurement  $U(\lambda) = 2u(\lambda)$  should be stated. The coverage probability for the coverage factor 2 then is 95%. The uncertainty of measurement thus is:

$$U(\lambda) = 2 \cdot (0.011) \text{ W} \cdot \text{m}^{-1} \cdot \text{K}^{-1} = 0.022 \text{ W} \cdot \text{m}^{-1} \cdot \text{K}^{-1}$$

In relative terms, this reads  $U'(\lambda) = (0.022/1.13) \cdot 100 = 1.9\%$ .

According to the GUM, the numerical value of the uncertainty is to be stated with two significant digits at most. The complete measurement result for this example is  $\lambda = (1.13 \pm 0.02) \text{ W} \cdot \text{m}^{-1} \cdot \text{K}^{-1}$ .

It is immediately apparent from Table III that the effect of the uncertainty in the power  $P_0$  measurement is negligible relative to the influence of the other quantities. The uncertainties in temperature measurements are the greatest.

Figure 2 presents the expanded uncertainty over the whole measurement range of the instrument analyzed. From its upper end at 6 to 0.1  $\text{W} \cdot \text{m}^{-1} \cdot \text{K}^{-1}$ , the uncertainty is almost constant. At the lower end of the range of 0.02  $\text{W} \cdot \text{m}^{-1} \cdot \text{K}^{-1}$ , the uncertainty increases to 2.9%.

To check the ability of the model presented, the uncertainty obtained was experimentally verified against the CRM 039 standard mentioned

Table III. Uncertainty Budget

Quantity $X_i$	Estimate $x_i$	Probability distrib.	Sensitivity coeff. $c_i = (\partial f(x)/\partial x_i)$	Stand. unc. $u(x_i)$	$u_i(y)$
$P_4$	3.9 W	normal	$1.27 \times 10^{-1} \text{ m}^{-1} \cdot \text{K}^{-1}$	$2.3 \times 10^{-6} \text{ W}$	$2.9 \times 10^{-1} \text{ W} \cdot \text{m}^{-1} \cdot \text{K}^{-1}$
$P_5$	0 W	normal	$1.27 \times 10^{-1} \text{ m}^{-1} \cdot \text{K}^{-1}$	$3.9 \times 10^{-6} \text{ W}$	$5.0 \times 10^{-1} \text{ W} \cdot \text{m}^{-1} \cdot \text{K}^{-1}$
$P_{51}$	0 W	normal	$-1.27 \times 10^{-1} \text{ m}^{-1} \cdot \text{K}^{-1}$	$9.2 \times 10^{-6} \text{ W}$	$-1.2 \times 10^{-1} \text{ W} \cdot \text{m}^{-1} \cdot \text{K}^{-1}$
$P_{52}$	0 W	normal	$-1.27 \times 10^{-1} \text{ m}^{-1} \cdot \text{K}^{-1}$	$9.2 \times 10^{-6} \text{ W}$	$-1.2 \times 10^{-1} \text{ W} \cdot \text{m}^{-1} \cdot \text{K}^{-1}$
$P_{53}$	0 W	normal	$-1.27 \times 10^{-1} \text{ m}^{-1} \cdot \text{K}^{-1}$	$9.2 \times 10^{-6} \text{ W}$	$-1.2 \times 10^{-1} \text{ W} \cdot \text{m}^{-1} \cdot \text{K}^{-1}$
$A_9$	$7853.98 \times 10^{-6} \text{ m}^2$	rectangular	$-1.44 \times 10^2 \text{ W} \cdot \text{m}^{-3} \cdot \text{K}^{-1}$	$7.9 \times 10^{-6} \text{ m}^2$	$-1.1 \times 10^{-1} \text{ W} \cdot \text{m}^{-1} \cdot \text{K}^{-1}$
$d_6$	$10 \times 10^{-3} \text{ m}$	rectangular	$1.13 \times 10^3 \text{ W} \cdot \text{m}^{-2} \cdot \text{K}^{-1}$	$5.0 \times 10^{-6} \text{ m}$	$5.8 \times 10^{-1} \text{ W} \cdot \text{m}^{-1} \cdot \text{K}^{-1}$
$dT_5$	10 K	normal	$1.13 \times 10^{-1} \text{ W} \cdot \text{m}^{-1} \cdot \text{K}^{-2}$	$5.7 \times 10^{-2} \text{ K}$	$6.4 \times 10^{-3} \text{ W} \cdot \text{m}^{-1} \cdot \text{K}^{-1}$
$dT_6$	0 K	normal	$1.13 \times 10^{-1} \text{ W} \cdot \text{m}^{-1} \cdot \text{K}^{-2}$	$5.7 \times 10^{-2} \text{ K}$	$6.4 \times 10^{-3} \text{ W} \cdot \text{m}^{-1} \cdot \text{K}^{-1}$
$dT_7$	0 K	normal	$1.13 \times 10^{-1} \text{ W} \cdot \text{m}^{-1} \cdot \text{K}^{-2}$	$5.7 \times 10^{-2} \text{ K}$	$6.4 \times 10^{-3} \text{ W} \cdot \text{m}^{-1} \cdot \text{K}^{-1}$
$\lambda$	$1.13 \text{ W} \cdot \text{m}^{-1} \cdot \text{K}^{-1}$				$0.011 \text{ W} \cdot \text{m}^{-1} \cdot \text{K}^{-1}$